Åbo Akademi University

Anna-Maria Brandt

PREDICTION OF 3D STRUCTURE AND LIGAND-BINDING PROPERTIES:

ABC transporters and flavodiiron proteins from *Synechocystis* sp. strain PCC 6803

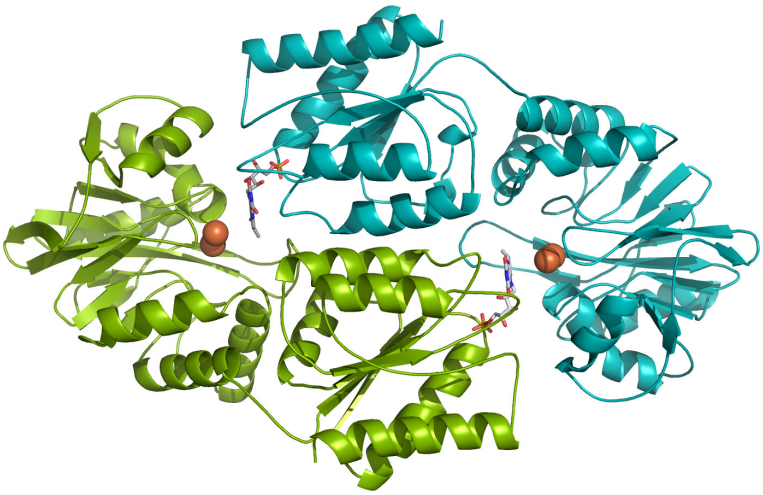

PREDICTION OF 3D STRUCTURE AND LIGAND-BINDING PROPERTIES:

ABC transporters and flavodiiron proteins from

Synechocystis sp. strain PCC 6803

Anna-Maria Brandt

Biochemistry
Department of Biosciences
Åbo Akademi University
Åbo, Finland
2013

Supervised by

Docent Tiina A. Salminen
Department of Biosciences
Åbo Akademi University
Turku, Finland

Reviewed by

Docent Olli Pentikäinen
Computational Bioscience Laboratory
Department of Biological and Environmental Science
University of Jyväskylä
Jyväskylä, Finland

Docent Esa Tyystjärvi
Molecular Plant Biology
Department of Biochemistry and Food Chemistry
University of Turku
Turku, Finland

Opponent

Professor Ramanathan Sowdhamini
National Center for Biological Sciences
Tata Institute of Fundamental Research
Bangalore, India

Cover: The overall fold of the Flv2/Flv4 heterodimer from *Synechocystis* with bound FMNs shown as sticks and irons shown as spheres.

ISBN 978-952-12-2886-5
Painosalama Oy , Turku 2013

Contents

List of original publications

This thesis is based on the following original publications, which are referred to by Roman numerals (I-IV) in the text.

I Anna-Maria Brandt*, Wuttinun Raksajit*, Paula Mulo, Aran Incharoensakdi, Tiina A. Salminen* and Pirkko Mäenpää* (2009) Transcriptional regulation and structural modeling of the FutC subunit of an ABC-type iron transporter in *Synechocystis* sp. strain PCC 6803. *Arch. Microbiol* **191**:561-70.

II Anna-Maria Brandt*, Wuttinun Raksajit*, Panutda Yodsang, Paula Mulo, Aran Incharoensakdi, Tiina A. Salminen and Pirkko Mäenpää (2010) Characterization of the substrate-binding PotD subunit in *Synechocystis* sp. strain PCC 6803. *Arch Microbiol* **192**:791-801.

III Panutda Yodsang, Wuttinun Raksajit, Anna-Maria Brandt, Tiina A. Salminen, Pirkko Mäenpää and Aran Incharoensakdi (2011) Recombinant polyamine-binding protein of *Synechocystis* sp. PCC 6803 specifically binds to and is induced by polyamines. *Biochemistry (Mosc)* **76**:713-9.

IV Pengpeng Zhang, Marion Eisenhut, Anna-Maria Brandt, Dalton Carmel, Henna M. Silén, Imre Vass, Yagut Allahverdiyeva, Tiina A. Salminen and Eva-Mari Aro (2012) Operon flv4-flv2 provides cyanobacterial photosystem II with flexibility of electron transfer. *Plant Cell* **24**:1952-71.

* Equal contribution to the work.

Contribution of the author

All multiple sequence alignments, homology modeling, database searches related to the modeling and structural analysis were performed by the author of this thesis. In publication III, the ligand docking was also performed by the author. The author wrote all sections regarding her own work in publications I-IV.

Other publications

Matti Lahti*, Eva Bligt*, Henri Niskanen, Vimal Parkash, Anna-Maria Brandt, Johanna Jokinen, Pekka Patrikainen, Jarmo Käpylä, Jyrki Heino and Tiina A. Salminen (2011) Structure of collagen receptor integrin α(1)I domain carrying the activating mutation E317A. *J Biol Chem* **286**:43343-51.

Mira Tulla, Matti Lahti, Santeri Puranen, Anna-Maria Brandt, Jarmo Käpylä, Anna Domogatskaya, Tiina A. Salminen, Karl Tryggvason, Mark S. Johnson and Jyrki Heino (2008) Effects of conformational activation of integrin α1I and α2I domains on selective recognition of laminin and collagen subtypes. *Exp Cell Res* **314**:1734-43.

*Equal contribution to the work

Acknowledgements

The work in this thesis was carried out at the Structural Bioinformatics Laboratory, Åbo Akademi University. Many people have helped me in my work and I want to express my gratitude to them.

First and most of all, I want to thank my excellent supervisor Docent Tiina Salminen for all her support and patience. You have always taken time to help and encourage me whatever problems I have had. I also want to express my gratitude to Professor Mark Johnson for all the support and, especielly, for feedback on this thesis. I have had the pleasure of belonging to the excellent National Doctoral Programme in Informational and Structural Biology (ISB), for which I thank Mark and coordinator Fredrik Karlsson.

I sincerely thank the reviewers, Docent Olli Pentikäinen and Docent Esa Tyystjärvi for the careful examination of my thesis.

The work in this thesis would not have been possible without collaboration. I want to acknowledge Professor Eva-Mari Aro, Dr. Pengpeng Zhang, Docent Pirkko Mäenpää, Dr. Wuttinun Raksajit and Dr. Panutda Yodsang for good collaboration.

I want to thank present and former members of the Structural Bioinformatics Laboratory, especially Lenita, the best travel companion ever, Heidi, Susanna, Yvonne, Tomi, Santtu, Eva and Käthe for the nice atmosphere in the lab. We have shared a lot of laughter both in and outside the lab. Thank you Jukka, for all the help with computer issues during the years, and Fredrik, for all the help with practical matters.

I would also like to acknowledge all the people at the Department of Biosciences for a nice working environment during the years. I especially want to thank Jessica, my dear friend, for all our discussions about work, life and our children. I am also grateful to the staff at the department, Elsmari Nyman, Pirkko Luoma and Juha-Pekka Sunila for helping me with many technical and practical matters during the years.

I want to express my deepest gratitude to my parents, Lena and Stig, who have let me choose my own path in life and always supported me.

Finally, I want to express my deepest love and gratitude to my family: Ari, you always encourage me and help me see the positive side of things. Linn and Rasmus, my love for you is never-ending.

Financial support from the National Doctoral Programme in Informational and Structural Biology (ISB), Sigrid Jusélius Foundation, Magnus Ehrnrooth

Foundation, the Swedish Cultural Foundation in Finland, the Finnish Cultural Foundation, Stiftelsens för Åbo Akademi forskningsinstitut, the Rector of Åbo Akademi University and Tor, Pentti and Joe Borgs Foundation is gratefully acknowledged.

Borgå, April 2013

Anna Brandt

Abbreviations

3D	Three-dimensional
aa	amino acid
ABC	ATP-binding cassette
ATP	Adenosine triphosphate
BLAST	Basic Local Alignment Search Tool
FAD	Flavin adenine dinucleotide
FDP	Flavodiiron protein
Flv	Flavoproteins
FMN	Flavin mononucleotide
Fut	Iron transporter
GTP	Guanosine triphosphate
Mal	Maltose transporter
MBP	Maltose binding protein
NAD^+	Nicotinamide adenine dinucleotide
NBD	Nucleotide-binding domain
NCBI	National Center for Biotechnology Information
PDB	Protein Data Bank
PIR	Protein Information Resource
Pot	Polyamine transporter
PQ	Plastoquinone
PSI	Photosystem I
PSII	Photosystem II
ROS	Reactive oxygen species
TrEMBL	Translated European Molecular Biology Laboratory

Abstract

Cyanobacteria are unicellular, non-nitrogen-fixing prokaryotes, which perform photosynthesis similarly as higher plants. The cyanobacterium *Synechocystis* sp. strain PCC 6803 is used as a model organism in photosynthesis research. My research described herein aims at understanding the function of the photosynthetic machinery and how it responds to changes in the environment. Detailed knowledge of the regulation of photosynthesis in cyanobacteria can be utilized for biotechnological purposes, for example in the harnessing of solar energy for biofuel production.

In photosynthesis, iron participates in electron transfer. Here, we focused on iron transport in *Synechocystis* sp. strain PCC 6803 and particularly on the environmental regulation of the genes encoding the $FutA_2BC$ ferric iron transporter, which belongs to the ABC transporter family. A homology model built for the ATP-binding subunit FutC indicates that it has a functional ATP-binding site as well as conserved interactions with the channel-forming subunit FutB in the transporter complex.

Polyamines are important for the cell proliferation, differentiation and apoptosis in prokaryotic and eukaryotic cells. In plants, polyamines have special roles in stress response and in plant survival. The polyamine metabolism in cyanobacteria in response to environmental stress is of interest in research on stress tolerance of higher plants. In this thesis, the *potd* gene encoding an polyamine transporter subunit from *Synechocystis* sp. strain PCC 6803 was characterized for the first time. A homology model built for PotD protein indicated that it has capability of binding polyamines, with the preference for spermidine. Furthermore, in order to investigate the structural features of the substrate specificity, polyamines were docked into the binding site. Spermidine was positioned very similarly in *Synechocystis* PotD as in the template structure and had most favorable interactions of the docked polyamines. Based on the homology model, experimental work was conducted, which confirmed the binding preference.

Flavodiiron proteins (Flv) are enzymes, which protect the cell against toxicity of oxygen and/or nitric oxide by reduction. In this thesis, we present a novel type of photoprotection mechanism in cyanobacteria by the heterodimer of Flv2/Flv4. The constructed homology model of Flv2/Flv4 suggests a functional heterodimer capable of rapid electron transfer. The unknown protein sll0218, encoded by the *flv2-flv4* operon, is assumed to facilitate the interaction of the Flv2/Flv4 heterodimer and energy transfer between the phycobilisome and PSII. Flv2/Flv4 provides an alternative electron transfer pathway and functions as an electron sink in PSII electron transfer.

1 Review of the literature

1.1 Introduction

During the course of evolution genes have been under constant change. Duplications have resulted in elongated polypeptide chains or new gene copies (Doolittle 1981). Local changes, such as substitutions, insertions or deletions, have altered the amino acid sequence that the genes encode. Thus, two initially identical gene copies may over time have evolved independently and adapted new functions (Doolittle 1981). Proteins that have evolved from a common ancestor are called homologs (Fitch 2000).

The 3D structure of a protein is crucial for the proteins function and has therefore been conserved. In homologous proteins, the structure is much more conserved than the protein sequence (Chothia and Lesk 1986; Johnson *et al.* 1994). Consequently, proteins with low sequence identity can have very similar structures, often more similar in the core of the structure than on the surface. Mutations most often occur in loop regions on the surface of the protein, while residues in the core of the protein vary much less (Chothia and Lesk 1986).

There are several methods to determine the 3D structure of a protein, X-ray crystallography, nuclear magnetic resonance (NMR) and electron microscopy being the most common. X-ray crystallography is the oldest of the methods, with the first protein structure reported in 1958 (Kendrew *et al.*), and because x-ray crystallography is well suited for structure determination of many kinds of proteins, from small molecules to large complexes, it is still a method of choice today. X-ray crystallography is, however, a time-consuming method, which relies on good-quality crystals. Expression, purification and crystallization of a protein can often be the bottle-neck of the method.

The number of known protein sequences in sequence databases (539 000 protein sequences in the Uniprot Knowledgebase, March 2013; http://www.uniprot.org/; Uniprot Consortium 2012) is enormous compared to the number of protein structures (83 000 protein structures in the Protein Data Bank, April 2013; http://www.pdb.org; Berman *et al.* 2000). Even though the experimental structure determination methods are faster and easier than before, computational structure prediction methods have gained an important role (Tramontano *et al.* 1998). Homology modeling is based on the knowledge that evolutionarily related proteins have similar structures (Chothia and Lesk 1986). The 3D structure of a protein can be predicted based on the known structure of a homologous protein. The process of homology modeling of a target sequence involves finding a suitable template structure for modeling, aligning the sequence of the template structure with the target sequence,

validating the sequence alignment and then the actual model building (Johnson *et al.* 1994; Tramontano *et al.* 1998). The sequence alignment is very important, because the quality of the model highly depends on the accuracy of sequence alignment (Tramontano *et al.* 1998). One misaligned residue can shift a part of the sequence in wrong position in regard to the template, resulting in an incorrect structural model. Therefore, all available information e.g. experimental data, functional residues and multiple alignments of family members of both target and template proteins should be taken advantage of in making the alignment (Tramontano *et al.* 1998).

The sequence similarity is lost more rapidly in evolution than the structural similarity. Therefore, there are no exact rule on what the similarity between a template and a target should be to make an accurate model. There are only some rules of thumb, which can be used: Doolittle (1990) have defined that protein sequences over a 100 residues long with a sequence identity over 25 % are very likely to be homologous, while sequences less than 15 % probably are not. Sequences in the range between 15 to 25 % sequence identity may still be homologous (Doolittle 1990). On the other hand, how accurate the models needs to be, also depends on the purpose for which the model will be used. Depending on the local sequence similarity of the region, reliability of the backbone structure and accuracy of the side-chain positions, there are regions in a homology model, which are more reliable and regions that are less reliable. Therefore, useful information can be obtained from the more reliable regions in a model, even though the model is based on a lower overall sequence identity (for review see Tramontano *et al.* 1998). The homology modeling process is further discussed in the Methods section.

Four proteins were studied in this thesis; the ferric iron transporter ATPase (FutC) and the polyamine transporter periplasmic binding protein (PotD) belong to the ABC transporter family, while Flv2 and Flv4 are flavodiiron proteins. All four proteins are from *Synechocystis* sp. PCC 6803 (hereafter *Synechocystis*), which is a unicellular non-nitrogen (N_2)-fixing cyanobacterium. The cyanobacteria are prokaryotes, which are able to perform oxygenic photosynthesis very similarly to higher plants. *Synechocystis* has been used extensively as a model organism for photosynthesis studies. The entire genome of *Synechocystis* was sequenced in 1996 as the first phototropic organism to be fully sequenced (Kaneko *et al.* 1996). The genome contains 3167 genes, of which 32 groups of genes potentially encode ABC-type transport systems (Ikeuchi and Tabata 2001). Several of these have been identified for a variety of substrates including metals, sugars and lipids. Therefore, *Synechocystis* also serves as a good model for analysis of ABC-type transport (Ikeuchi and Tabata 2001).

1.2 ABC transporters

The ATP-binding cassette (ABC)-ATPase superfamily is one of the largest paralogous protein families (Higgins 1992). The superfamily consists of two subfamilies: modular transporters that, driven by hydrolysis of ATP, import or export molecules across the cytoplasmic membrane and ABC proteins that are located in the cytosol or nucleus and are involved in the regulation of cellular processes such as DNA repair, translation and gene expression (Doolittle *et al.* 1986; Higgins 1992). In this thesis, the focus will be on the ABC transporter subfamily. ABC transporters are present in almost all living cells (Higgins 1992) and their substrates range from small molecules such as ions, sugars or amino acids to large compounds such as lipids, oligopeptides and drug molecules (Moussatova *et al.* 2008). Generally, the ABC transporters are relatively specific for their substrates and there is an ABC transporter for most different types of molecules that need to cross the cellular membrane. Despite the extreme diversity of their substrates, the ABC transporters share a common structure of two transmembrane channel-forming subunits and two cytoplasmic nucleotide-binding domains (NBD). The channel-forming subunits have unrecognizable sequence identity and vary in length, architecture, and number of transmembrane helices (from 6-20) (Moussatova *et al.* 2008).

1.2.1 ABC transporter structures

The NBD is responsible for the hydrolysis of ATP and is highly conserved. The NBD consists of a RecA-like subdomain and a helical subdomain, which are found in all available NBD structures (Figure 4A in publication I). Some ATPases also contain a regulatory domain, like in the sulfate transporter ATPase CysA from *Alicyclobacillus acidocaldarius* (Scheffel *et al.* 2005), the glucose transporter ATPase GlcV from *Sulfolobus solfataricus* (Verdon *et al.* 2003) and the maltose transporter ATPase MalK from *Escherichia coli* (Chen *et al.* 2003). All NBDs contain several conserved sequence motifs involved in either ATP-binding or in forming of the dimer (Figure 1) (Hollenstein *et al.* 2007b). In the RecA-like subdomain, the Walker A (also called P-loop) and Walker B motifs bind the nucleotide. The Walker A motif is rich in glycine residues (Gly-X-X-Gly-X-Gly-Lys-Ser/Thr), while the Walker B motif contains a conserved glutamate residue. The helical subdomain contains the LSGGQ motif (the ABC signature motif), which binds the ATP from the opposite monomer in the dimer. The Q-, D- and H-loops complete the ATP-binding site and are involved in the catalytic cycle (George and Jones 2012). The Q-loop is involved in making contact to the transmembrane domain, and the D-loop is involved in contact mediating at the interface of the dimer. A conserved glutamate at the junction of the Walker B motif and the D-loop is proposed to act as the catalytic base with the nucleophilic water during ATP hydrolysis, while the histidine in the H-loop is proposed to be involved in forming the catalytic dyad together with the

glutamate (Jones and George 2012). Additionally, the A-loop contains an aromatic residue, which stacks against the adenine moiety of the bound ATP (Ambudkar *et al.* 2006; Hollenstein *et al.* 2007b).

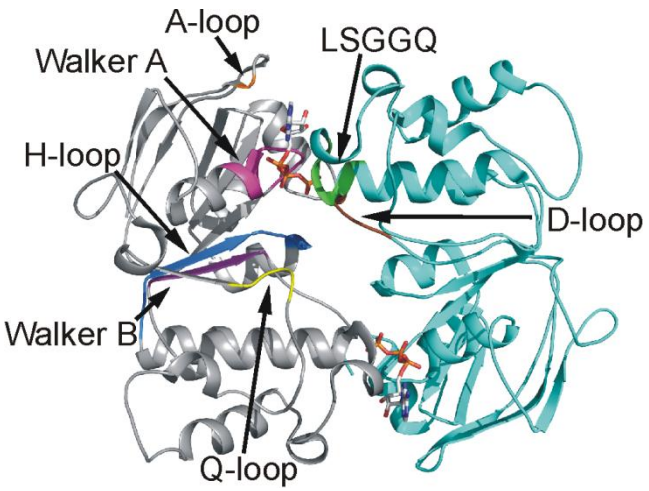

Figure 1. The NBDs of MalK from *E. coli* (PDB ID: 1Q12, Chen *et al.* 2003). One monomer is colored cyan, the other gray with structural motifs highlighted. The ATP binding sites are in the interface between the monomers, with bound ATP molecules shown as sticks. The regulatory domains are not shown.

In bacteria, ABC transporters are divided into prokaryotic-type and eukaryotic-type ABC transporters (Moussatova *et al.* 2008). The eukaryotic-type transporters expressed in bacteria are exporters, such as multidrug transporters conferring drug resistance to the cell. They are able to recruit substrates directly from the cytoplasm. Prokaryotic-type transporters, on the other hand, are importers utilizing substrate binding proteins to bind the substrates from the extracellular space and shuttle them to the transporter (Moussatova *et al.* 2008). In Gram-negative bacteria these are called periplasmic binding proteins. The transporters in my work belong to prokaryotic-type transporters, which will be discussed in more detail.

To date, twelve crystal structures of intact ABC transporters have been determined: vitamin B_{12} transporter BtuCD from *E. coli* (Locher *et al.* 2002), multidrug transporter Sav1866 from *Stafylococcus aureus* (Figure 2) (Dawson and Locher 2006, 2007), multidrug transporter MsbA from *Vibrio cholera*, *E. coli* and *Salmonella typhimurium* (Ward *et al.* 2007), molybdate/tungsten transporter ModBC from *Archaeoglobus fulgidus* and *Methanosarcina acetivorans* (Hollenstein *et al.* 2007a; Gerber *et al.* 2008), metal-chelate-type transporter HI1470/71 from *Haemophilus influenzae* (Pinkett *et al.* 2007), the methionine transporter MetNI of *E. coli* (Kadaba *et al.* 2008), the murine P-glycoprotein (Aller *et al.* 2009), TM287/288 from *Thermotoga maritima* (Hohl

et al. 2012) and the maltose transporter $MalFGK_2$ from *E. coli*, which has been determined in the *apo* and ATP-bound states (Oldham *et al.* 2007; Oldham and Chen 2011a) (Figure 2). The TM287/288 from *Thermotoga maritima* and the three multidrug transporters Sav1866, MsbA and P-glycoprotein are ABC-type exporters.

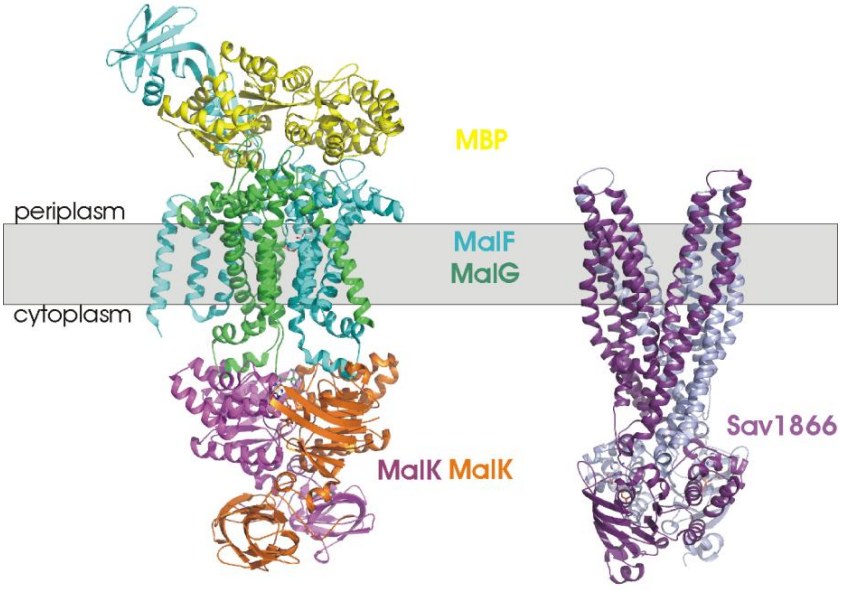

Figure 2. Crystal structures of $MalFGK_2$ and Sav1866. MalFGK is the maltose importer complex in *E. coli* (PDB ID: 3RLF, Oldham and Chen 2011b). Sav1866 is a multidrug transporter, which exports diverse cytotoxic drugs across cell membranes in *S. aureus* (PDB ID: 2HYD, Dawson and Locher 2006).

The 3D structures of intact ABC transporters give some insight into the transport mechanism. The "ATP switch model" (Figure 3) is a dynamic model for coupling of ATP hydrolysis and substrate transfer using the maltose transporter as an example (Higgins and Linton 2004; Oldham *et al.* 2011a). Maltose diffuses through the outer membrane via maltoporin into the periplasm. The maltose binding protein (MBP) binds maltose and interacts in the closed conformation with the resting state $MalFGK_2$ (Figure 3). When MBP binds to the $MalFGK_2$ the NBDs are brought closer to each other and the transmembrane subunits are reorientated causing the MBP to open. This outward-facing conformation allows transfer of maltose from MBP to the transmembrane subunit binding site and simultaneously places ATP at the catalytic site for hydrolysis. Once ATP is hydrolyzed the subunits most likely reorient towards the cytoplasm and the substrate is released into the cytoplasm. The crystal structure of the complete transporter after ATP hydrolysis is, however, still lacking (Oldham and Chen 2011a, 2011b).

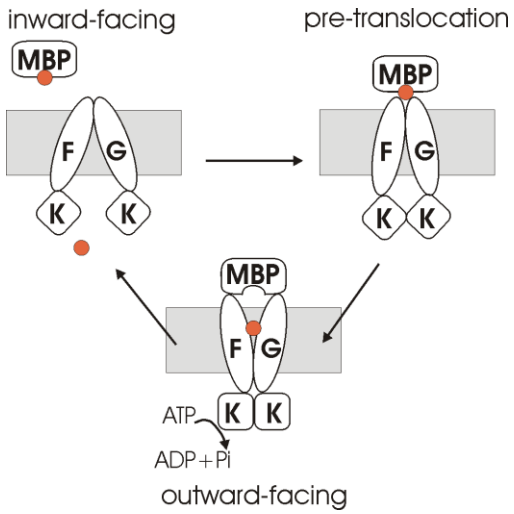

Figure 3. The "ATP switch model". After entering the periplasm, maltose is bound to the MBP. MBP interacts with the inward-facing $MalFGK_2$, which transforms into the pre-translocation conformation. In the pre-translocation conformation, binding of MBP brings the NBDs closer to each other causing large conformational changes: MalK closure, rotation of MalFG and opening of MBP. In the outward-facing conformation, maltose is transferred to its binding site on MalFG and, simultaneously, ATP is positioned at the catalytic site for hydrolysis. Once ATP is hydrolyzed, the MalFG reorients towards the cytoplasm and maltose is released into the cell (Adapted from Oldham and Chen 2011a).

1.2.2 Iron transport

Iron is an essential poorly soluble nutrient, for which organisms have developed special uptake systems. Iron can exist either in an oxidized ferric form Fe(III) or in a reduced ferrous form Fe(II), which is unstable under aerobic conditions (Kranzler *et al.* 2011). Host proteins, such as transferrin, lactoferrin, and ferritin, bind iron. Iron uptake systems for transferrin, lactoferrin, hemoglobin and siderophores have been identified in both Gram-negative and Gram-positive bacteria (Krewulak and Vogel 2008).

Siderophores are low molecular weight, high-affinity iron chelators, which scavenge ferric iron from the extracellular environment (Krewulak and Vogel 2008). Siderophores vary widely in overall structure, but they are classified according to their functional groups, which coordinate iron, as catecholates, hydroxymates, hydroxypyridonates, or aminocarboxylates (Stinzi *et al.* 2000).

The uptake systems require an outer membrane receptor for uptake into the periplasmic space, a periplasmic binding protein and an inner membrane receptor. In *E. coli*, four outer membrane receptors have been characterized:

the ferrichrome receptor (FhuA), the ferric citrate receptor (FecA), the ferric enterobactin receptor (FepA), and the iron aerobactin receptor (IutA). The crystal structure has been determined for three of them: FhuA (Locher *et al.* 1998), FecA (Ferguson *et al.* 2002) and FepA (Buchanan *et al.* 1999). All three structures share a similar fold consisting of a β-barrel of 22 antiparallel strands with an N-terminal globular domain, called the cork or plug. As the outer membrane in Gram negative bacteria lacks an ion gradient or ATP hydrolysis mechanism, the energy needed for iron transport across the outer membrane is supplied by the TonB-ExbB-system (Krewulak and Vogel 2008). The TonB-ExbB-system couples the inner membrane electrochemical potential to the outer membrane receptors via three proteins: TonB, ExbB and ExbD. The periplasmic binding protein brings the siderophores to the inner membrane receptor for transport to the cytoplasm. In *E. coli* FhuD, FecB and FepB are responsible for binding hydroxamate, ferric citrate and catechol-type siderophores, respectively (Krewulak and Vogel 2008). Each periplasmic protein internalizes the siderophore into the cytoplasm via their own respective transporter. The crystal structures of FhuD with various siderophores revealed a common binding mechanism; two highly conserved key residues (Tyr106 and Arg84) that form hydrogen bonds with the siderophores in the structures (Clarke *et al.* 2000, 2002). The inner membrane receptors belong to the ABC transporters, which are described in section 1.1.2.

Siderophore transport has been shown in many cyanobacterial species and studied in detail in *Anabena* sp. strain PCC 7120 (Nicolaisen *et al.* 2008). However, siderophore biosynthesis genes have not been found in *Synechocystis*, *Prochlorococcus* and *Synechococcus* species (Ehrenreich *et al.* 2005), suggesting an alternative iron uptake system. *Synechocystis* has been shown to acquire iron both from exogenous ferrisiderophore complexes and inorganic iron by reduction before transport across the plasma membrane (Kranzler *et al.* 2011).

Transferrin and lactoferrin are glycoproteins with the molecular mass of about 80 kDa and they contain two high-affinity Fe(III) binding sites. Both of them are too large to cross the outer membrane and, therefore, iron needs to be extracted before transport to the periplasm (Krewulak and Vogel 2008). In many pathogenic bacteria, the extraction is performed by outer membrane proteins (TbpA/TbpB, LbpA/LbpB), which are predicted to bind to the transferrin or lactoferrin and force the domains surrounding the iron binding site apart from each other, thereby releasing the iron (Schryvers and Stojiljkovic 1999). After transfer to the periplasm, the iron is bound by ferric binding proteins, FbpA, which brings it to the FbpB/FbpC cytoplasmic membrane transporter (Schryvers and Stojiljkovic 1999). Crystal structures of the FbpA from *Neisseria* sp., *Haemophilus influenzae* and *Pasteurella*

haemolytica have been solved both in *apo* and in *holo* forms (Bruns *et al.* 1997, 2001; Shouldice *et al.* 2003a, 2003b). The FbpA structure is very similar to one lobe of transferrin, having two similarly folded domains and the iron binding site located between the domains.

When iron is scarce microorganisms must use all source of iron available. E. g. heme from hemoglobin can be used as an iron source by some microorganisms. Patogenic bacteria excrete exotoxins, such as hemolysins (Stoebner and Payne 1988), cytolysins (Lagergard *et al.* 1993) and proteases (Simpson and Oliver 1993) that lyse the cell and release the heme. Two mechanisms for acquiring heme have been identified in Gram negative bacteria (Perkins-Balding *et al.* 2004; Wandersman and Delepelaire 2004). The first mechanism involves direct uptake of heme or heme associated with host hemoproteins, such as haptoglobin, albumin, hemoplexin, or myoglobin. The heme is aquired by a TonB-dependent outer membrane receptor, a periplasmic binding protein and an ABC transporter (Bracken *et al.* 1999). For example, heme receptors HpuA/HpuB (Rohde *et al.* 2002) and HmbR (Stojiljkovic *et al.* 1996) have been identified in *Neisseria meningitidis*. The second mechanism involves bacterial proteins, hemophores, to extract the iron from heme. In *Serratia marcescens*, the hemophore HasA (Izadi *et al.* 1997; Arnoux *et al.* 1999, 2000) tightly binds heme and delivers it to the outer membrane receptor HasR, which is a β-barrel receptor composed of 22 anti-parallell β-strands (Krieg *et al.* 2009). The crystal structure of HasR in complex with hemophore HasA gives insight into the transfer mechanism of heme into the periplasm (Krieg *et al.* 2009). Heme is translocated through the outer membrane by HasR in an active transport process coupled with the TonB-complex, which derives energy from the electrochemical potential of the cytoplasmic membrane (Letoffe *et al.* 2004). In the periplasm, heme binds to a heme binding protein, which shuttles the heme molecule to an ABC transporter for transport across the cytoplasmic membrane.

Another type of iron uptake system, which has been characterized in many plants, yeast and eukaryotic algae reduces ferric iron (Fe^{3+}) to more soluble ferrous iron (Fe^{2+}) via a plasma membrane redox system before transporting it (Lesuisse and Labbe 1989; Morrissey and Guerinot 2009). For example, some algal species use ferric chelate reductase to reduce iron and symbiotic organisms such as root bacteria to import ferrous iron (King and Garey 1999). *E. coli* also has a Fe(II) transport system encoded by *feoA*, *feoB* and *feoC* (Kammler *et al.* 1993). Fe(II) diffuses across the outer membrane via undefined porins and is then transported in an ATP/GTP-driven process across the cytoplasmic membrane by the Feo system (Cartron *et al.* 2006).

1.2.3 Iron transporters in *Synechocystis*

Several genes involved in iron transport have been identified in the *Synechocystis* genome, for example *feoB*, which belongs to the ferrous iron transport system (Katoh *et al.* 2000, 2001). Experiments showed that when the *feoB* gene was inactived, Fe(II) uptake was impaired in *Synechocystis* and that the *feoB* system is induced by low intracellular iron concentrations (Katoh *et al.* 2001). The $FutA_2BC$ transporter, consisting of substrate-binding subunits FutA1 and FutA2, a membrane associated subunit FutB and an ATP-binding subunit FutC was identified as the major iron transporter in *Synechocystis.* FutA1 and FutA2 has been shown to bind unchelated Fe(III) (Katoh *et al.* 2001; Badarau *et al.* 2008). $FutA_2BC$ is related to the transferrin and lactoferrin associated iron transporter systems Sfu in *S. marcescens* (Angerer *et al.* 1990) and Fbp in *Neisseria gonorrhoeae* (Berish *et al.* 1990).

The crystal structures of the substrate-binding subunits FutA1 and FutA2 in *Synechocystis* have been determined both in the presence and absence of bound iron (Koropatkin *et al.* 2007; Badarau *et al.* 2008). The sequence identity shared by *Synechocystis* FutA1 and FutA2 is 52 % and the FutA2 structure is very similar to the FutA1 structure (Badarau *et al.* 2008). Both bind iron in a similar manner, via four tyrosine and one histidine residues. The changes in the structure upon iron binding and release are similar in FutA1 and FutA2. FutA2 is the most abundant soluble iron-binding protein in the periplasm of *Synechocystis* (Fulda *et al.* 2000) and is likely to be the primary ferric-binding protein in the iron transporter of *Synechocystis* (Badarau *et al.* 2008). FutA1 is present in the thylakoid membrane (Tölle *et al.* 2002; Srivastava *et al.* 2005), the plasma membrane (Huang *et al.* 2002) and the outer membrane (Huang *et al.* 2004). The phenotypes of FutA1 deletion mutants suggest a role in protection of photosystem II under iron limiting conditions in *Synechocystis* (Tölle *et al.* 2002; Michel and Pistorius 2004).

In this thesis, an aim was to characterize the iron transporter $FutA_2BC$ in *Synechocystis*. Based on sequence alignments and a homology model we show that the ATP-binding subunit FutC is well conserved and has a completely functional ATP binding site. Moreover, the association of FutC to the transmembrane subunits is also conserved.

1.2.4 Polyamine transport

Polyamines (putrescine, cadaverine, spermidine, and spermine) are polycationic molecules, which are found in nearly all procaryotic and eukaryotic cells. Polyamines contain two or more primary amino groups. Putrescine is the smallest and spermine the largest polyamine (Figure 9 on page 38). Polyamines are involved in various cellular processes such as

regulation of cell proliferation, differentiation and apoptosis (Heby *et al.* 1981, Packham and Cleveland 1994, Thomas and Thomas 2001, Seiler and Raul 2005). Due to their ability to interact with negatively-charged molecules, polyamines are involved in the stabilization of DNA, RNA, chromatin and proteins. As polyamines stimulate cell growth they are also associated with embryonic development, various types of cancer and parasite-related infection. In plants, polyamines are involved in the response to stress and diseases, indicating their importance for plant survival (Bouchereau *et al.* 1999; Groppa and Benavides 2008; Kusano *et al.* 2008).

In *E. coli* and very recently in *Pseudomonas aeruginosa*, polyamine ABC transporters have been structurally characterized (Igarashi and Kashiwagi 1999; Wu *et al.* 2012). *E. coli* contains two polyamine uptake systems; one for spermidine-preferential uptake (PotABCD) (Furuchi *et al.* 1991) and another for putrescine-specific uptake (PotFGHI) (Pistocchi *et al.* 1993) (Figure 5). The polyamine transporters consist of four subunits: the periplasmic binding protein (PotD or PotF), two transmembrane proteins (PotB and PotC or PotH and PotI) and an ATPase (PotA or PotG) (Igarashi and Kashiwagi 1999; Igarashi *et al.* 2001). The crystal structures of *E. coli* PotD and PotF in the ligand-bound form have been solved (Sugiyama *et al.* 1996a; Vassylyev *et al.* 1998).

The polyamine transporter in *P. aeruginosa* (SpuDEFGH) consists of the periplasmic substrate binding proteins SpuD and SpuE (Figure 4), the channelforming proteins SpuH and SpuG, and the ATPase SpuF (Lu *et al.* 2002). SpuD preferentially binds putrescine, while SpuE specifically binds spermidine. The crystal structures of SpuD and SpuF have recently been solved in the *apo* and ligand-bound forms (Wu *et al.* 2012). Additionally, the crystal structure of TpPotD from the spirochetal bacterium responsible for causing syphilis, *Treponema pallidum*, has been solved with 2-(*N*-morpholino)-ethanesulfonic acid (MES) bound to the ligand binding site (Machius *et al.* 2007).

The structure of *E. coli* PotD consists of two domains with an $\beta-\alpha-\beta$ topology, which is a typical fold for periplasmic binding proteins (Sugiyama *et al.* 1996a). In the substrate binding site, which is buried in a pocket between the two domains, three residues (Glu171, Trp255 and Asp257) were crucial for binding spermidine, while five residues (Trp34, Tyr85, Asp168, Trp229 and Tyr293) had moderate importance and five other residues had weak contribution to the binding of spermidine (Kashiwagi *et al.* 1996; Sugiyama *et al.* 1996b). The crystal structure of *E. coli* putrescine-specific PotF is very similar to that of PotD, with a similar substrate binding cleft between the two domains (Vassylyev *et al.* 1998). In addition to the residues that are crucial for binding putrescine in PotF (Trp37, Ser85, Glu185, Trp244, Asp247 and Asp278), a water molecule was also found be important for binding. The presence of the water molecule in the binding cleft of PotF creates a barrier for putrescine, which in

absence of the water would be able to penetrate deeper into the binding cleft and shift the binding mode. PotD preferentially binds spermidine, but is also able to bind putrescine with a lower affinity. Among the 13 spermidine binding residues in PotD, seven are conserved in PotF (Trp37, Tyr40, Ser85, Glu185, Trp244, Asp278 and Tyr314).

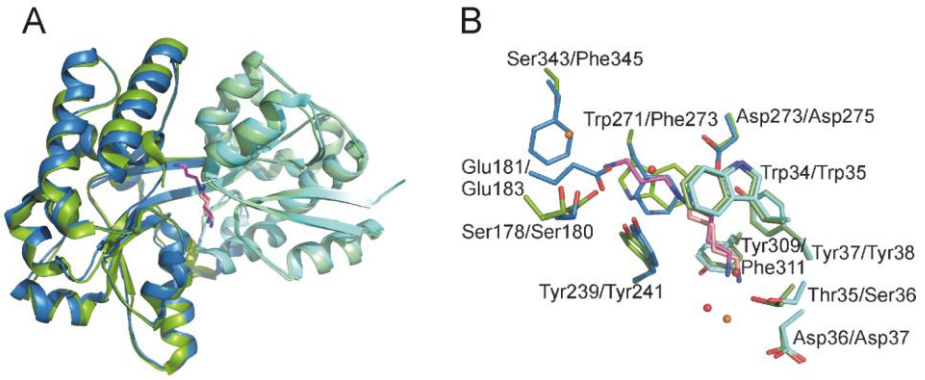

Figure 4. The crystal structures of SpuD with bound putrescine and SpuE with bound spermidine superimposed on top of each other (PDB ID: 3TTM (SpuD), 3TTN (SpuE); Wu *et al.* 2012). (A) SpuD: N-terminal domain (light cyan), C-terminal domain (blue) and putrescine (light pink); SpuE: N-terminal domain (light green), C-terminal domain (green) and spermidine (magenta). (B) The polyamine binding sites in SpuD and SpuE. Waters in the SpuD structure are shown in red and in the SpuE structure in orange. Residue numbering: SpuE/SpuD.

Residues involved in spermidine recognition have been identified in the transmembrane subunits PotB and PotC of the polyamine transporter (Higashi *et al.* 2010). Residues at the periplasmic side (Leu110 in PotB and Asp198 and Asp199 in PotC) are probably involved in releasing spermidine from PotD for transport across the membrane and residues at the cytoplasmic side (Tyr261 in PotB and Asp108 in PotC) are involved in releasing spermidine together with ADP into the cytoplasm (Higashi *et al.* 2010). The PotA dimer is associated with the membrane through PotB and PotC. PotA couples the energy from ATP hydrolysis to the transport of polyamines. The ATP binding pocket (Cys26, Phe27, Phe45, Cys54, Leu60, and Leu76) and residues necessary for the interaction with another PotA (Cys26) and PotB (Cys54) are located in the N-terminal domain. The ATPase activity was inhibited by spermidine, suggesting that spermidine functions as a feedback inhibitor of transport (Kashiwagi *et al.* 2002).

Other polyamine transporters identified in *E. coli* are putrescine transporter PotE (Kashiwagi *et al.* 1991; Tomitori *et al.* 2001) and cadaverine transport system CadB (Soksawatmaekhin *et al.* 2004) (Figure 5). Both PotE and CadB are

membrane proteins consisting of 12 transmembrane segments and function as antiporters. PotE functions as an antiporter for putrescine/ornithine and CadB for cadaverine/lysine (Kashiwagi *et al.* 1992, 1997, 2000; Soksawatmaekhin *et al.* 2004; Tomitori *et al.* 2012). A spermidine excretion system MdtJI was recently identified in *E. coli* (Higashi *et al.* 2008). MdtJ and MdtI consist of four transmembrane segments each and their functional residues are situated at the cytoplasmic side of the membrane in a similar manner as for PotE and CadB. Additionally, a putrescine utilization pathway in *E. coli* has been identified, which includes a putrescine importer gene *puuP* (Kurihara *et al.* 2005).

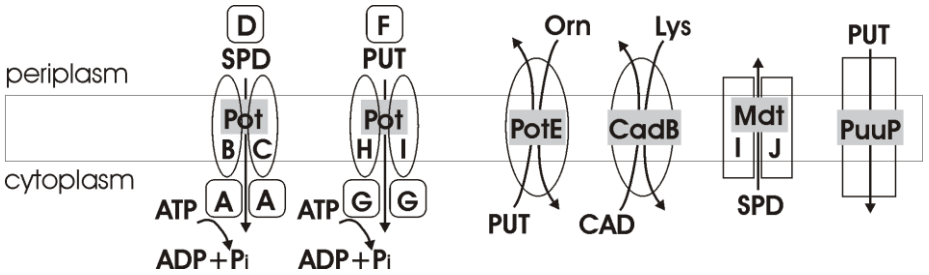

Figure 5. Polyamine transporters in *E. coli*. Adapted from Igarashi and Kashiwagi, 2010.

1.2.5 Polyamine transport in *Synechocystis*

The gene encoding a periplasmic binding protein for spermidine/putrescine (PotD, *slr0401*) was identified based on sequence similarity in the genome of *Synechocystis* (Kaneko *et al.* 1996). When the uptake of polyamines was studied in *Synechocystis*, the existence of a putrescine transport system was recognized (Raksajit *et al.* 2006). Furthermore, putrescine uptake was strongly inhibited by ATPase inhibitors indicating that the uptake is ATP-dependent. The transport was also inhibited by spermidine and spermine, suggesting a common transport system (Raksajit *et al.* 2006). Spermidine uptake experiments, on the other hand, showed that transport was specific for spermidine, with noncompetitive inhibition by putrescine and spermine. Spermidine uptake was also shown to be energy-dependent (Raksajit *et al.* 2009). These results led to the characterization of the *Synechocystis potd* gene. The function and substrate preference of the *Synechocystis* periplasmic binding protein PotD were studied using homology modeling and ligand docking. In this thesis, the results indicated that PotD has a conserved overall fold and that it is able to bind polyamines. Furthermore, by combining molecular docking with *in vitro* as well as *in vivo* binding studies we showed that PotD prefers spermidine over putrescine or spermine.

1.3 Flavodiiron proteins

Flavodiiron proteins are a large family of enzymes involved in protection of the cell against the toxicity of oxygen and/or nitric oxide (Vicente *et al.* 2008a). The active site of oxygen reduction is the non-heme diiron binding site, which is positioned close to the cofactor, flavin mononucleotide (FMN), in a head-to-tail dimer formation of the protein. *Synechocystis* encodes four flavodiiron proteins (Flv1-4) (Vicente *et al.* 2008a). Flavodiiron proteins can form homodimers or homotetramers. However, Flv1 and Flv3 from *Synechocystis* were recently shown to function as a heterodimer (Allahverdiyeva *et al.* 2011). In this thesis, the aim was to characterize the function and location of Flv2 and Flv4. In my work, I investigated by homology modeling whether they could form functional heterodimers with each other and, moreover, studied the diiron and FMN-binding sites predicted in the models.

1.3.1 Photosystem II

During oxygenic photosynthesis, carbohydrates are formed from H_2O and CO_2 by water oxidation and carbon dioxide reduction (Dau *et al.* 2012). Oxygenic photosynthesis takes place in the chloroplasts, which are organelles found in plant cells and in cyanobacteria. The light-dependent reactions take place in the thylakoid membrane (Dau *et al.* 2012). Solar energy is used to transfer electrons from water to $NADP^+$ via the three multisubunit chlorophyll-protein complexes: photosystem II (PSII), cytochrome b6f and photosystem I (PSI). ATP synthase generates ATP by using the electrochemical gradient generated across the thylakoid membrane during electron transport. PSII is located in the the thylakoid membrane of cyanobacteria, algae and terrestrial plants (Dau *et al.* 2012; Yin *et al.* 2012). However, the cyanobacterium *Gloeobacter violaceus* lacks the thylakoid membrane and instead the photosynthetic apparatus is found in the cytoplasmic membrane (Rexroth *et al.* 2011).

Several crystal structures of cyanobacterial PSIIs have been solved (Zouni *et al.* 2001; Kamiya and Shen 2003; Ferreira *et al.* 2004; Guskov *et al.* 2009), the most recent from *Thermosynechococcus vulcanus* at 1.9 Å resolution (PDB ID: 3ARC, Umena *et al.* 2011) (Figure 6). PSII is formed by a dimeric core with 17 intrinsic and three extrinsic protein subunits per monomer, 35 chlorophylls, two pheophytins, eleven β-carotenes, 2 plastoquinones, 2 haems, 1 non-haem iron and a number of ions (Umena *et al.* 2011). In the center of the PSII core complex is the D1 and D2 heterodimer, with the light-harvesting CP47 and CP43 proteins on each side. The light is captured by chlorophyll at the surface of the antenna proteins CP47 and CP43. In cyanobacteria, phycobilisomes are the major light-harvesting proteins. The light energy is transferred to P680, which is the primary electron donor. P680, in turn transfers one electron to a pheophytin, which is a chlorophyll molecule lacking the central Mg^{2+} ion and

functions as primary electron acceptor. A charge separation is stabilized by fast electron transfer to plastoquinone (Q_A) resulting in the formation of cationic radical $P680^+$. The secondary plastoquinone (Q_B) accepts two electrons and two protons forming a plastoquinol (PQH_2). PQH_2 enters the PQ pool in the thylakoid membrane, which provides the connection between PSII and the cytochrome b6f complex. PQH_2 is re-oxidized to plastoquinon-9 (PQ) and returns to PSII, whereas the reduction equivalents are transferred to PSI. A redox-active D1-Tyr161 reduces the radical $P680^+$ by receiving electrons from the Mn_4Ca cluster at the lumenal side of PSII. After four steps of one-electron oxidation of the Mn_4Ca complex dioxygen is formed (reviewed in Aro *et al.* 1993; Nixon *et al.* 2010; Komenda *et al.* 2012).

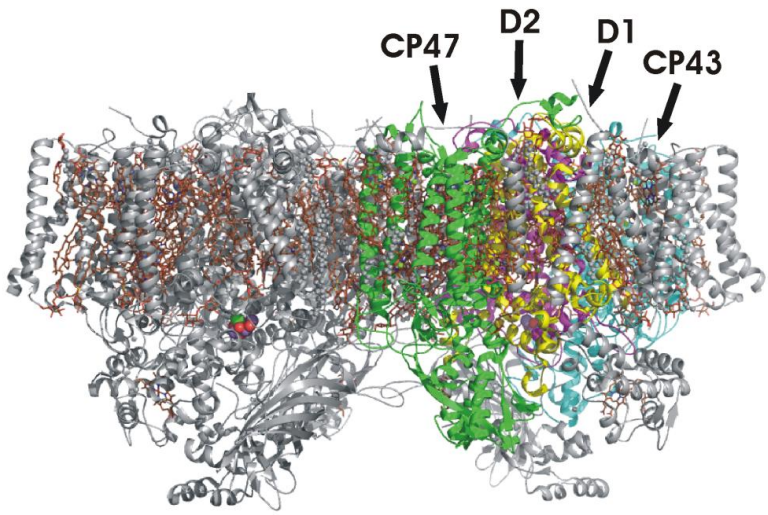

Figure 6. PSII from *Thermosynechococcus vulcanus* at 1.9 Å (PDB ID: 3ARC, Umena *et al.* 2011). In the right hand monomer D1 and D2 protein are coloured magenta and yellow, respectively. CP47 and CP43 are coloured green and cyan, respectively. The left hand monomer is colored grey. The Mn_4CaO_5 clusters are shown as spheres. The cofactors are colored brown.

1.3.2 Photoprotection of PSII

The light-induced irriversible damage to the photosynthetic apparatus is referred to as photoinhibition (reviewed in Tyystjärvi 2013). Photosynthetic organisms have developed protective mechanisms to balance the absorption and utilization of light energy (reviewed in Niyogi 1999). Adjustment of the size of the light-harvesting antenna, alternative electron transport pathways and release of excess heat are examples of the protective mechanisms that plants utilize. Additionally, a wide variety of antioxidant molecules and scavenging enzymes take care of the reactive molecules formed, especially the reactive oxygen species (ROS). Despite these photoprotective mechanisms, light-

induced irreversible damage still occurs and the PSII activity is a constant balance between damage and repair of the PSII centers. The PSII repair cycle is an important photoprotective mechanism in all oxygenic photosynthetic organisms because it replaces damaged proteins, mainly D1, by synthesizing new protein (reviewed in Nixon *et al.* 2005, 2010). If the repair is not efficient enough, damaged PSII starts accumulating. During the repair cycle PSII is partly disassembled, the damaged subunits are degraded and the newly synthesized subunits are incorporated in the PSII.

Members of the FtsH and Deg protease families are involved in degradation of damaged D1. Studies with *Synechocystis* FtsH showed that FtsH alone is able to efficiently degrade and synthesize D1, without the prior cleavage of Deg proteases (Silva *et al.* 2003; Nixon *et al.* 2005). According to the model of the repair cycle including only FtsH, damage to D1 triggers partial disassembly of the dimeric PSII (Nixon *et al.* 2010). During disassembly PSII forms a monomeric complex (RC47). The hexameric FtsH2/FtsH3 complex removes D1 from the membrane in a process driven by ATP hydrolysis. While damaged D1 is degraded, newly synthesized D1 is inserted into the RC47 complex to minimize destabilization of RC47 (Nixon *et al.* 2010). The mechanism behind the insertion of newly synthesized D1 is not known. Studies in *Synechocystis* suggest a post-translational insertion, while studies in chloroplasts point towards co-translational replacement (Komenda *et al.* 2006; Zhang *et al.* 1999). Finally, the intact dimeric PSII is reassembled. Even if Deg proteases are not essential for D1 degradation in *Synechocystis*, in chloroplasts the Deg proteases facilitate and accelerate the FtsH mediated degradation of D1 by cleaving interhelical loops, thereby preventing the formation of ROS (Nixon *et al.* 2010). Flavodiiron proteins in *Synechocystis* have been shown to play an important role in protection of PSII against photoinhibition, and they will be discussed in detail in following chapters.

1.3.3 Flavodiiron protein structure

Flavodiiron proteins (FDPs), also called A-type flavoproteins (Flvs), are a large family of enzymes involved in detoxification of O_2 and NO in strict and facultative anaerobic bacteria and archaea as well as in pathogenic protozoa (Vicente *et al.* 2008b). The FDPs show different substrate selectivity, even though they are structurally similar. *E. coli* flavorubredoxin has a preference for NO, while *Moorella thermoacetica*, *Desulfovibrio gigas* and *Desulfovibrio vulgaris* FDPs have both O_2 and NO reductase activity (Vicente *et al.* 2008c). *Methanothermobacter marburgensis* and *Methanobrevibacter arboriphilus* FDPs, on the other hand, reduce O_2 to water exclusively (Seedorf *et al.* 2004, 2007). The protozoan FDPs from *Giardia intestinalis* and *Trichomonas vaginalis* are also selective towards O_2 (Di Matteo *et al.* 2008; Smutna *et al.* 2009).

The crystal structures of many FDPs have been solved (Frazão *et al.* 2000; Silaghi-Dumitrescu *et al.* 2005; Seedorf *et al.* 2007; Di Matteo *et al.* 2008). The typical enzyme core consists of two conserved domains: the β-lactamase-like domain, which contains a diiron center, and the flavodoxin domain, which contains a flavin mononucleotide (FMN) binding site. The β-lactamase-like domain has a structurally very similar fold as class B Zn-β-lactamases (Carfi *et al.* 1995) and human glyoxylase (Cameron *et al.* 1999), despite the low sequence identity. In FDPs, the metal active site is a nonheme diiron center, while lactamases contain mono- and dizinc centers and glyoxylases contains iron-zink binuclear centers (Cameron *et al.* 1999; Zang *et al.* 2001). Two monomers are in a head-to-tail arrangement in the dimeric structures, bringing the diiron site and the FMN-binding site of opposite monomers together (Figure 7A). The FDP substrates are small (O_2/NO) and can reach the diiron site easily, while lactamases and glyoxylases have bulky substrates, which require large cavities next to their metal sites (Vicente *et al.* 2008a).

The C-terminal flavodoxin domain has a typical α–β–α fold and shares significant structural similarity with short-chain flavodoxins (Frazão *et al.* 2000). The FDPs have, however, a higher FMN reduction potential than the flavodoxins due to the relative excess of basic versus acidic residues surrounding the FMN isoalloxazine ring in FDPs (Gomes *et al.* 1997; Silaghi-Dumitrescu *et al.* 2003; Vicente and Teixeira 2005). Previous studies have shown that FDPs form homodimers and homotetramers (Frazão *et al.* 2000, Silaghi-Dumitrescu *et al.* 2005, Seedorf *et al.* 2007, Di Matteo *et al.* 2008), however, we showed in publication IV that *Synechocystis* Flv2 and Flv4 are able to form heterodimers.

Some exceptions in the common two-domain arrangement have been found: In *E. coli* flavorubredoxin, a rubredoxin domain has been fused to the C-terminal end of the core structure. The rubredoxin domain contains a FeS center, which is able to reduce sulphate (Wasserfallen *et al.* 1998; Gomes *et al.* 2000). Another example is the rubredoxin from *M. thermoacetica*, which has a NAD(P)H:flavin oxidoreductase domain fused to an N-terminal rubredoxin domain. This NAD(P)H:flavin oxidoreductase domain is the putative redox partner of the *M. thermoacetica* FDP, both encoded at the same operon (Das *et al.* 2001).

In cyanobacterial and some photosynthetic eukaryotic FDPs, an additional flavin reductase domain is found at the C-terminal end of the proteins (Vicente *et al.* 2002; Zhang *et al.* 2009). The domain binds FMN or flavin adenine dinucleotide (FAD). In *Synechocystis* the flavin reductase domain uses NAD(P)H as an electron donor. Therefore, *Synechocystis* Flv is capable of linking NADH oxidation to oxygen reduction, thereby condensing a reaction, which requires

three proteins in *Desulfovibrio gigas* (Gomes *et al.* 1997), two in *E. coli* (Gomes *et al.* 2000), and one protein in *Synechocystis* (Vicente *et al.* 2002).

1.3.4. The diiron center and the FMN binding site

The diiron center is the active site of O_2/NO reduction and globally conserved. The mechanism behind the substrate preference is, however, not completely clear. In most structures each iron is coordinated by two imidazole nitrogens, two oxygens from carboxylate residues and by a solvent molecule (Vicente *et al.* 2008a). In *Desulfovibrio gigas* rubredoxin:oxygen oxidoreductase, the proximal iron, the iron closer to the FMN, is coordinated by His79, His146, and Glu81, while the distal iron, further away from the FMN, is coordinated by His84, His226 and Asp83 (Frazão et al. 2000). Asp165 acts as the bridging ligand for both iron atoms. Each iron has a fifth coordination position, where the substrate can bind (Vicente *et al.* 2008a).

The structure of *Methanothermobacter marburgensis* $F_{420}H_2$ oxidase was solved both in reduced and oxidized forms, which revealed large differences between the two forms (Seedorf et al. 2007) (Figure 7). In the oxidized form the distal iron maintains its coordination, while the proximal iron is displaced. The rotation of Glu81 creates a new metal-binding site and, additionally, a third putative metal-binding site is found at the protein surface. As a consequence of the displacement of the proximal iron, the loop consisting of residues 148-151 (*M. marburgensis* $F_{420}H_2$ oxidase numbering), called the switch loop, is rearranged. This, in turn, leads to increased accessibility of the redox centers (Seedorf et al. 2007).

All FDP structures solved so far contain an FMN binding site (Vicente *et al.* 2008a). The structural motifs that bind the FMN in *D. gigas* rubredoxin:oxygen oxidoreductase (Frazão et al. 2000), *M. marburgensis* $F_{420}H_2$ oxidase (Seedorf et al. 2007) (Figure 7B and 7C) and *M. thermoacetica* FprA (Silaghi-Dumitrescu et al. 2005) are well conserved. As the FMN binding site is located at the monomer interface, it becomes shielded from solvent in the dimer. FMN is bound by van der Waals interactions and hydrogen bonds between FDP and the isoalloxazine ring of the FMN. FDP structures contain a conserved tryptophan residue stacked with its indole group against the isoalloxazine ring of the FMN, protecting FMN from the solvent (Vicente *et al.* 2008a). The tryptophan is replaced by a glycine residue in some FDPs, for example in *M. marburgensis* $F_{420}H_2$ oxidase. In the oxidized form of the *M. marburgensis* $F_{420}H_2$ oxidase structure, the open conformation of the switch loop together with the small glycine residue results in a space large enough to allow parallel docking of $F_{420}H_2$ next to the FMN (Figure 7C). The parallel docking allows direct electron transfer between the $F_{420}H_2$ and FMN (Pejchal *et al.* 2005; Warkentin *et al.* 2001). The tryptophan residue found in most FDPs obstructs

the protein from receiving electrons directly from a co-factor; instead electrons are accepted from other redox proteins, typically rubredoxins. The tryptophan residue is exclusively replaced by a glycine in FDPs from methanogens and cyanobacteria (Vicente *et al.* 2008a).

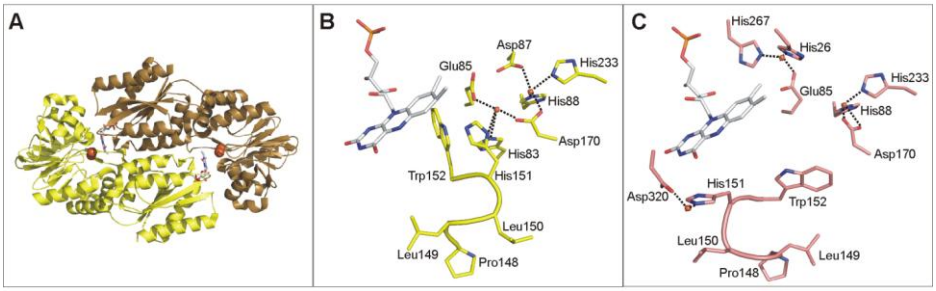

Figure 7. The overall structure of *M. marburgensis* $F_{420}H_2$ oxidase (A) and the active site in closed (B) and open (C) conformations. FMNs are shown in light gray and irons in orange. (PDB ID: 2OHI (closed conformation), 2OHJ (open conformation); Seedorf *et al.* 2007).

1.3.5 Flvs in *Synechocystis* sp. strain PCC 6803

In *Synechocystis*, four genes (*sll1521*, *sll0219*, *sll0550* and *sll0217*) encoding Flv proteins (Flv1, Flv2, Flv3 and Flv4, respectively) have been identified. Flv2 and Flv4 are unique for cyanobacteria, while homologous proteins for Flv1 and Flv3 can be found in green algae, mosses and *Selaginella* (Zhang *et al.* 2009). Flv homologs have, however, not been identified in higher plants. Analysis of all available cyanobacterial genomes showed that there are at least two genes encoding Flvs in each organism (Zhang *et al.* 2009). A phylogenetic analysis (Figure 8) show that the genes were divided into two clusters (FlvA and FlvB) with one copy in each cluster. Each cluster is divided into four subclusters. The FlvA cluster divides into eukaryotic FlvA, α-cyanobacteria FlvA, β-cyanobacteria Flv1 and β-cyanobacteria Flv2 subclusters. The FlvB cluster divided into eukaryotic FlvB, α-cyanobacteria FlvB, β-cyanobacteria Flv3 and β-cyanobacteria Flv4 subclusters. The four *Synechocystis* Flv genes were found in the FlvA and FlvB β-cyanobacteria branches, divided into Flv1, Flv2, Flv3 and Flv4 subclusters, respectively. *Nostoc punctiforme* and *Anabaena* contains five and six genes encoding Flvs, respectively. These genes were found as pairs in the subclusters, indicating multiple isoforms in the genome (Zhang *et al.* 2009).

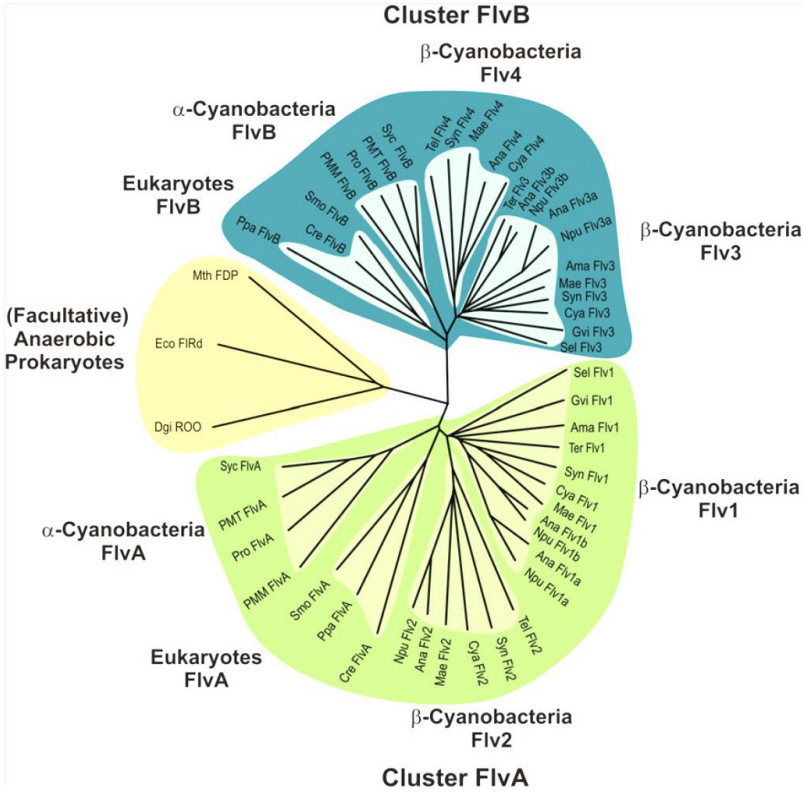

Figure 8. Phylogenetic analysis of flavodiiron proteins in anaerobes, facultative aerobes and oxygenic photosynthetic organisms (reprinted from Zhang *et al.* 2009).

The Mehler´s reaction was discovered in 1951 in spinach leaves by A.H. Mehler (Mehler 1951). During the reaction, O_2 is reduced to superoxide (O_2^-), which is rapidly converted into H_2O_2 by superoxide dismutase enzyme. A Mehler-like reaction in cyanobacteria directly reduces O_2 to water without producing ROS, while in eukaryotes the reaction leads to the formation of free O_2 radicals (Helman *et al.* 2003). Biochemical analysis showed that Flv3 is a NAD(P)H:oxygen oxidoreductase, capable of reducing O_2 to water *in vitro* (Vicente *et al.* 2002). Flv1 and Flv3 were shown to function in the Mehler reaction in *Synechocystis* and provide an efficient means to remove excess energy in the photosynthetic apparatus. Only the Flv1/Flv3 heterodimer is physiologically functional in the Mehler-like reaction *in vivo* (Allahverdiyeva *et al.* 2011).

Accumulation of ROS have been shown to inhibit the synthesis of D1 and the repair of damaged PSII centers (Nishiyama *et al.* 2006). In a study with inactivation mutants of *flv2* and *flv4*, Zhang *et al.* (2009) showed that the degradation rate of the D1 protein was faster in the *flv2* and *flv4* inactivation mutants than in wild-type and that the repair of damaged PSII was slowed

down too. This indicated a important role for Flv2 and Flv4 in preventing the production of ROS and furthermore, in protecting PSII against photoinhibition (Zhang *et al.* 2009).

2 Aims of study

In publication I, the aim was to study the transcriptional regulation of the previously uncharacterized iron transporter *futA$_2$BC* in *Synechocystis*. The transporter ATPase FutC was studied at the protein level and homology modeling was done to permit study of the overall structure and ATP binding of FutC. Furthermore, the contact of FutC to the transmembrane subunit FutB was examined.

Publication II describes the characterization of the *Synechocystis potd* gene at the transcript and protein levels. The aim was to study whether *potd* is a functional gene and if PotD protein is able to bind polyamines. The multiple sequence alignment and homology model of PotD were constructed to study whether the substrate binding site is conserved and to analyze the polyamine binding properties.

In publication III, the aim was to study polyamine binding by recombinant PotD protein from *Synechocystis*. Substrate docking was done to study the structural determinants for the polyamine binding specificity and, moreover, provide an explanation for the spermidine preference.

In publication IV, the aim was to characterize the function of the *flv4-flv2* operon encoding Flv4, sll0218 and Flv2 proteins in *Synechocystis*. Homology modeling was carried out to study whether *Synechocystis* Flv2 and Flv4 are capable of forming functional heterodimers and to examine the formed binding sites. Moreover, we wanted to clarify how the proposed heterodimer would associate with the membrane.

3 Methods

3.1 Sequence and structure databases

The protein sequences and structures used in this thesis were obtained from web-based databases. Protein sequences were obtained from the Uniprot Knowledgebase (http://www.uniprot.org/; Uniprot Consortium 2012), the genome database at the National Center for Biotechnology Information (NCBI, http://www.ncbi.nlm.nih.gov/) and Cyanobase (http://genome.kazusa.or.jp/cyanobase; Nakao *et al.* 2010). Cyanobase is the genome database for cyanobacteria. The Uniprot Knowledgebase (Uniprot Consortium 2012) is a protein sequence database combining information from the former Swiss-Prot, Translated European Molecular Biology Laboratory (TrEMBL) and Protein Information Resource (PIR) database. The Uniprot Knowledgebase (Uniprot Consortium 2012) contains manually and computationally annotated protein sequences with information about the amino acid sequence, taxonomy, biological function as well as cross-references to other databases.

Protein structures were retrieved from the Protein Data Bank (PDB, http://www.pdb.org; Berman *et al.* 2000). The PDB contains information about the structures of proteins, nucleic acids and the complex assemblies determined by x-ray crystallography, nuclear magnetic resonance (NMR), cryoelectron microscopy and neutron diffraction.

Basic Local Alignment Search Tool (BLAST, http://www.ebi.ac.uk/Tools/sss/ncbiblast/) was used for sequence searches of the Uniprot Knowledgebase (Uniprot Consortium 2012) and PDB (Berman *et al.* 2000). BLAST finds regions of local similarity in protein sequences and reports the statistical significance of matches between the query sequence and protein sequences in the databases.

3.2 Sequence alignment

In order to more easily recognize the conserved areas of the target sequence, multiple sequence alignments were made including homologous structures as well as sequences. The multiple sequence alignments were manually refined, before a pairwise alignment was derived for modeling. Sequence alignments were constructed with MALIGN (Johnson and Overington 1993) and structure-based sequence alignments were constructed by superimposing crystal structures with VERTAA (Johnson and Lehtonen 2000). Both programs are included in the BODIL visualization and modeling package (Lehtonen *et al.* 2004).

In publication I, the structures were obtained from the PDB (Berman *et al.* 2000): MalK from *E. coli* (PDB ID: 1Q12), MalK from *Thermococcus litoralis* (PDB ID: 1G29), multiple sugar-binding transport ATPase from *Pyrococcus horikoshii* (PDB ID: 2D62), CysA from *Alicyclobacillus acidocaldarius* (PDB ID: 1Z47) and GlcV from *Sulfolobus solfataricus* (PDB ID: 1OXV) were retrieved for a structure-based multiple sequence alignment. The sequence of FutC from *Synechocystis* was combined to the alignment and the alignment was then manually refined (Figure 4b in publication I). A pairwise alignment of FutC from *Synechocystis* and the template structure MalK from *E. coli* was derived for modeling.

In publication II, a multiple sequence alignment (Supplementary fig. S1 in publication II) consisting of cyanobacterial ABC transporter polyamine binding subunits was constructed (Table 1). The structures of *E. coli* PotD and PotF were superimposed and combined with the sequence alignment. Secondary structure predictions were used to support the alignment (PredictProtein, Rost *et al.* 2004). A pairwise alignment of *Synechocystis* PotD and *E. coli* PotD was derived for modeling.

Table 1. Sequences of polyamine binding subunits included in the sequence alignment

Code	Putative protein	Species	Seq. ID %
slr0401 [1]	PotD	*Synechocystis*	
YP_722480 [2]	Periplasmic polyamine-binding protein of ABC transporter	*Trichodesmium erythraeum*	45
alr0299 [1]	ABC transporter, periplasmic polyamine-binding protein	*Nostoc sp. PCC7120*	41
tll0716 [1]	Hypothetical protein	*Thermosynechococcus elongatus*	40
syc1832_d [1]	Periplasmic polyamine-binding protein of ABC transporter	*Synechococcus sp. PCC7942*	37
NP_219092 [2]	Spermidine/putrescine ABC transporter, periplasmic binding protein (potD)	*Treponema pallidum subsp. pallidum str. Nichols*	18
1POT [3]	PotD	*E. coli*	24
1A99 [3]	PotF	*E. coli*	19

[1] Cyanobase
[2] NCBI
[3] PDB

In publication IV, a structure-based sequence alignment of the β-lactamase and flavodoxin domains (Supplemental Figure 6 in publication IV) was constructed by superposing five crystal structures (Table 2) and aligning them to *Synechocystis* Flv2 and Flv4. The crystal structures were identified by BLAST search of the PDB using Flv2 and Flv4 as query sequences. The sequence alignment was refined based on the structures and a multiple sequence

alignment consisting of Flv2 and Flv4 and 22 putative cyanobacterial flavoprotein sequences, which were identified by a BLAST search of the Uniprot Knowledgebase (Uniprot Consortium 2012). The pairwise sequence alignments needed for modeling Flv2 and Flv4 were derived from the multiple sequence alignment.

The flavin reductase domains of Flv2 and Flv4 from *Synechocystis* were used as query sequences in BLAST searches of the PDB (Berman *et al.* 2000). A multiple structure-based alignment of the flavin reductase domains (data not shown) was created based on the retrieved structures and *Synechocystis* Flv2 and Flv4 flavin reductase domains.

Table 2. Crystal structures of FDPs that were used in the structure-based alignment together with the sequences of Flv2 and Flv4

PDB ID	Protein	Species
2OHI	$F_{420}H_2$ oxidase, closed conformation	*Methanothermobacter marburgensis*
2OHJ	$F_{420}H_2$ oxidase, open conformation	*Methanothermobacter marburgensis*
1YCF	FprA	*Moorella thermoacetica*
1E5D	Dioxygen reduction enzyme	*Desulfovibrio gigas*
2Q9U	Flavodiiron protein	*Giardia intestinalis*
1VME	Flavoprotein	*Thermotoga maritima*

A BLAST search of the PDB (Berman *et al.* 2000) was conducted with sll0218 as the query sequence. A multiple sequence alignment with sll0218 and 13 cyanobacterial homologs, all unknown proteins, was created (data not shown). To aid the refinement of the alignment, a secondary structure prediction of sll0218 was performed with PSIPRED (http://bioinf.cs.ucl.ac.uk/psipred/; Jones 1999; Buchan *et al.* 2010) and included in the alignment. A prediction of transmembrane helices was made by TMHMM (http://www.cbs.dtu.dk/services/TMHMM/; Krogh *et al.* 2001).

3.3 Homology modeling

Homology modeling is a method for constructing an estimated 3D structure for a protein sequence based on the known crystal structure of a homologous protein. The model is created based on a sequence alignment of the target protein and the template structure. The accuracy of the alignment is of great importance, since the quality of the model is dependent on it.

The homology models were constructed with MODELLER (Sali and Blundell 1993). MODELLER automatically calculates a model containing all non-hydrogen atoms based on a template structure and a pairwise sequence

alignment of the target protein and the template protein. A set of ten models was created and the model with the best MODELLER objective function was chosen for further analysis. The models were evaluated by PROCHECK (Laskowski *et al.* 1993). All homology models were superimposed on template structures with VERTAA (Johnson and Lehtonen 2000) and visually examined.

In publication I, the homology model of FutC from *Synechocystis* (Figure 5 in publication I) was modeled as a dimer based on the crystal structure of the ATP-bound form of *E. coli* MalK (PDB ID:1Q12) and a pairwise alignment of FutC and MalK derived from the multiple sequence alignment (Figure 4b in publication I). Two ATP molecules were included in the model.

The *Synechocystis* PotD model in publication II and III (Figure 1a in publication II) was modeled based on *E. coli* PotD crystal structure (PDB ID: 1POT) and a pairwise alignment of *Synechocystis* PotD and *E. coli* PotD derived from the multiple sequence alignment (Supplementary fig. S1 in publication II) of cyanobacterial polyamine binding subunits (Table 1). Spermidine and a conserved water molecule were included in the active site. The stereochemistry and the fold of the model were evaluated with PROCHECK (Laskowski *et al.* 1993) and PROSA2003 (Sippl 1993), respectively. A surface loop (Ala83-Thr102) was excluded from the model since the template structure did not have information on residues in this region.

In publication IV, homology models for the β-lactamase-like and flavodoxin domains of *Synechocystis* Flv2 and Flv4 were created both in heterodimeric (Figure 8A in publication IV) and homodimeric forms. The open and closed conformations were constructed based on the crystal structure of $F_{420}H_2$ oxidase from *M. marburgensis* (closed conformation, PDB ID: 2OHI; open conformation, PDB ID: 2OHJ) and a multiple sequence alignment (Supplemental Figure 6 in publication IV), from which pairwise alignments were derived, respectively. A model of the Flv2/Flv4 heterodimer in the closed conformation was also constructed based on FprA *from Moorella thermoacetica* (PDB ID: 1YCF) and the alignment.

The C-terminal flavin reductase domains of Flv2 and Flv4 were modeled separately, because structures with all three domains (β-lactamase, flavodoxin and flavin reductase domains) have not been solved so far. Three-dimensional models of the Flv2 and Flv4 flavin reductase domains (Figure 8C in publication IV) were constructed based on the crystal structure of *Archaeoglobus fulgidus* ferric reductase (PDB ID: 1I0S) and pairwise sequence alignments derived from a multiple sequence alignment (data not shown) of Flv2 and Flv4 flavin reductase domains and sequences in Table 2. The structure of *A. fulgidus* ferric reductase contains bound FMN and NADH. FMN was included in the binding sites of the Flv2 and Flv4 flavin reductase domain models.

3.4 Ligand docking

Ligand docking is a computer-based method for prediction of the best fit of a ligand to the binding site in a protein. The program searches for the best position for a small molecule in the binding site and the number of favorable interactions (hydrogen bonds, hydrophobic interactions) between the ligand and protein are evaluated by a scoring function.

The ligands in publication III were drawn in Sybyl 8.0 (Tripos International, USA). The ligands were docked into the homology model of PotD (publication II). The spermidine molecule in the homology model was removed and hydrogens were added in Sybyl 8.0 (Tripos International, USA). In the putrescine docking experiment, the conserved water molecule, which is involved in binding putrescine in *E. coli* PotF (PDB ID: 1A99) was included prior to adding hydrogens. For the docking experiments GOLD 3.2 (Jones *et al.* 1995, 1997) was used. It uses a genetic algoritm as a search algoritm and allows full ligand flexibility. Ten independent runs with default docking parameters were made. The binding sites were restricted within 15 Å radius of the central oxygen: Asp206-OD2 in the spermidine and spermine docking experiments and Asp295-OD2 in the putrescine docking experiment. The docking was stopped if the three best docking results were within an rmsd of 1.5 Å.

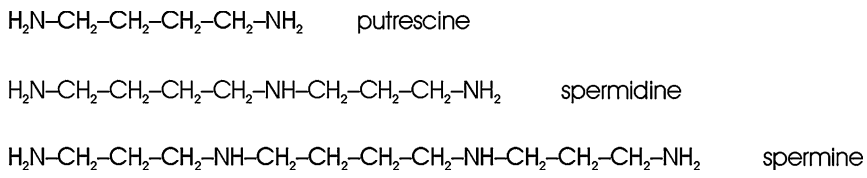

Figure 9. Polyamines used in the docking experiment.

4 Results and discussion

4.1 The ABC transporters

The ABC transporters have been the subject of extensive research during the past 20 years. A great number of crystal structures are available for the substrate binding subunits and, recently, crystal structures of several full ABC transporters have also been solved (Locher *et al.* 2002; Dawson and Locher 2006, 2007; Hollenstein 2007a; Oldham *et al.* 2007; Pinkett *et al.* 2007; Ward *et al.* 2007; Gerber *et al.* 2008; Kadaba *et al.* 2008; Aller *et al.* 2009; Oldham and Chen 2011a; Hohl *et al.* 2012). So far, relatively little is known about ABC transporters in the cyanobacterium *Synechocystis*. The aim of our work was to characterize the function of PotD, the substrate binding subunit of the polyamine transporter, and FutC, the ATPase of the iron transporter. At the gene level, we studied the environmental regulation of transcription and at the protein level, the predicted structures and ligand binding. We modeled the 3D structures of PotD and FutC in order to study the overall fold and their binding properties to obtain a better understanding of their function.

4.2 The homology model of FutC from *Synechocystis* sp. strain PCC 6803

In publication I, the transcriptional regulation of the genes *futA1*, *futA2*, *futB* and *futC*, encoding the iron uptake system in *Synechocystis*, was studied. Additionally, we modeled *Synechocystis* FutC in order to analyze its ATP-binding properties. The ABC-transporter ATPases have a highly conserved structure implying a common evolutionary origin and the family is distinguished from other ABC transporters by characteristic motifs (LSGGQ, Walker A, Walker B, Q loop), which interact with ATP.

Regulation of the $FutA_2BC$ transporter at the transcriptional level in response to environmental stresses was studied by the co-workers. The *futC* transcript, as well as the *futA1*, *futA2* and *futB* transcripts, showed a rapid increase in steady-state transcript levels when exposed to the environmental stresses tested (darkness, an alternative nitrogen source (NH_4Cl), unoptimal temperature, salt and osmotic stresses as well as iron deficiency) (Figures 2 and 3 in publication I). The increase in the steady-state transcript levels of *futC* was only transient, since the amount of transcript was downregulated 30 min after the treatment. Cyanobacteria face alterations in their environment, which require quick adjustments of gene function. The short-term regulation of the iron transporter genes indicate that *Synechocystis* is able to quickly respond to the altered conditions.

Sequences in the multiple sequence alignment (Figure 4b in publication I) showed 31-34 % sequence identity with *Synechocystis* FutC. Given the conserved nature of the structural fold among the ABC-type ATPases, MalK from *E. coli* was chosen as the template. MalK has the highest overall sequence identity, 34 %, with *Synechocystis* FutC. However, the nucleotide-binding domain (NBD) showed a significantly higher sequence identity, 45 %, compared to the regulatory domain (RD), which only showed 18 % sequence identity. The NBD comprises the RecA-like domain and a α-helical subdomain with the ABC family signature motif (LSGGQ). The RecA domain houses the nucleotide-binding site consisting of the conserved Walker A, Walker B and switch motifs (Figure 4b in publication I).

The ATP-binding sites are located at the interface between the FutC monomers (Figure 5 in publication I). The Walker A motif from one monomer binds the ATP-molecule by forming hydrogen bonds and van der Waals interactions with the nucleotide, while the LSGGQ motif stabilizes the binding from the other monomer. Of the 18 amino acids involved in the binding of ATP in *E. coli* MalK, 14 residues are totally conserved and four substituted by similar residues in *Synechocystis* FutC (Figure 10 and Figure 6 in publication I). A strong hydrogen bond is formed with the nucleotide by His192 in *E. coli* MalK, which is located in the H-loop (Chen *et al.* 2003) and corresponds to His215 in *Synechocystis*. Another important residue for nucleotide binding is Trp13 in *E. coli* MalK, which is replaced by Phe28 in *Synechocystis* FutC. A conserved aromatic residue (tryptophan, phenylalanine or tyrosine) at the corresponding position in human, plant, fungal and bacterial ABC transporter ATPases have been shown to be critical for nucleotide binding (Ambudkar *et al.* 2006).

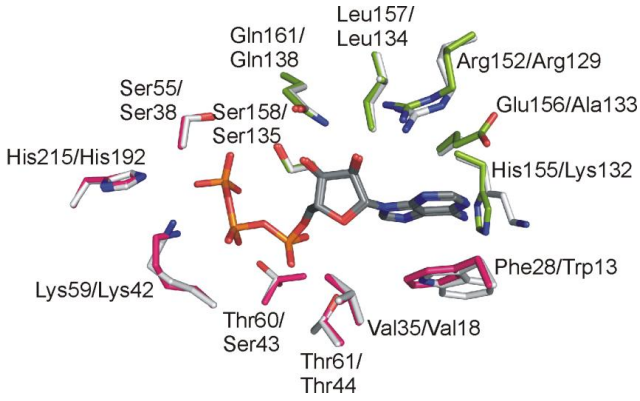

Figure 10. The ATP-binding sites of *Synechocystis* FutC and *E. coli* MalK (PDB ID: 1Q12, Chen *et al.* 2003) superimposed on top of each other. In *Synechocystis* FutC, residues from monomer A are coloured pink and residues from monomer B are coloured green. Residues from *E. coli* MalK are coloured light gray. The ATP molecules are in the middle. Residue numbering FutC/MalK.

We also wanted to analyze the potential interaction site of FutC with the transmembrane protein FutB. Analysis of the FutB sequence showed that it is divided into two homologous domains (aa 61-269 and 339-545) similar to the transmembrane subunit FhuB of the siderophore transport system (Groeger and Köster, 1998). FhuB-like transmembrane subunits have also been found in *Vibrio cholerae*, *Rhizobium leguminosarum*, and *Rhodobacter capsulatus* (Köster 2001). The crystal structure of the complete *E. coli* maltose transporter complex was recently determined and gave insight into the interaction at the MalK-MalF/MalG interface (Oldham *et al.* 2007). The channel-forming proteins MalF and MalG contain two short helices at the interface, which protrude into a hydrophobic pocket in MalK. The EAA motif in the coupling helices in MalF/MalG bind to MalK by forming salt bridges between the glutamate in the EAA loop and Arg47 in MalK (Oldham *et al.* 2007). The corresponding residue is also arginine (Arg64) in *Synechocystis* FutC. We found conserved regions EAS (aa 182-184) and DAA (aa 457-459) in FutB, which might be the contact loops. Thus, FutC may contact FutB via similar interactions. Additionally, other contacts between the coupling helices in MalK and MalG/MalF were observed: the side chains of Met405 in MalF and Leu194 in MalG inserts into a hydrophobic pocket on MalK formed by residues Ala50, Leu52, Ala73, Val77, Met79 and Phe81 (Oldham *et al.* 2007). In FutB the corresponding residue is Leu187 and the hydrophobic pocket of FutC is formed by residues Ala67, Phe69, Glu94, Thr98, Met100, Phe102. Coupling helices are also present in ModB, Sav1866, BtuCD, HI1470/71, which indicates a common hydrophobic interaction mechanism (Hollenstein *et al.* 2007a).

4.3 The homology model of PotD from *Synechocystis* sp. strain PCC 6803

In publications II and III, I studied the capability of *Synechocystis* PotD to bind polyamines by analyzing the active site of the created homology model as well as by docking substrates to the predicted binding site. Our co-workers confirmed by experimental work that PotD is capable of binding polyamines *in vitro* and *in vivo*.

The *Synechocystis* PotD model (Figure 1a in publication II) represents the closed spermidine-bound form of the periplasmic binding protein. Although the sequence identity between the periplasmic binding proteins can be low due to different substrate specificities, they all belong to the same structural family and share a typical α/β type fold (Sugiyama *et al.* 1996a). The sequence identity between the PotD template structure from *E. coli* and *Synechocystis* PotD was only 24 %, but the identity of residues within 8 Å of the binding site was noticeably higher (38%). The sequence identities of *Synechocystis* PotD with *E. coli* PotF and TpPotD were only 19 % and 18 %, respectively. The major

differences between the *E. coli* PotD structure and the model of *Synechocystis* PotD included a longer loop that would be located at the surface of the PotD model, which was left out of the model (aa Ala83-Thr102,) and a longer loop at the N-terminus, which can be seen in the model (Figure 1a in publication II).

E. coli PotF is specific for putrescine, while *E. coli* PotD is able to bind both spermidine and putrescine, but has a preference for spermidine. In *E. coli* PotD, thirteen residues have been reported to be important for binding spermidine and three of these (Glu171, Trp255 and Asp257) are crucial for ligand binding (Table 3) (Igarashi and Kashiwagi 1999). The three corresponding residues are conserved and equivalently positioned in our *Synechocystis* PotD model (Glu209, Trp267 and Asp295) as well as in *E. coli* PotF (Glu185, Trp244 and Asp278). In addition, two other spermidine binding residues are conserved between *E. coli* PotD (Asp168 and Trp229), and *Synechocystis* PotD (Asp205 and Trp293), creating the polyamine binding site. In conclusion, the polyamine binding site of *Synechocystis* PotD is more similar to the binding site of the spermidine-preferential *E. coli* PotD, than to the putrescine binding site of *E. coli* PotF.

Table 3. Residues lining the polyamine binding site in *E. coli*, *P. aeruginosa, T. pallidum* and *Synechocystis* proteins. The substrate preference is indicated (SPD; spermidine, PUT; putrescine, SPD/PUT; prefers spermidine, binds also putrescine, PUT/SPD; prefers putrescine, binds also spermidine) and conserved residues indicated by colored background.

E. coli **PotD**	***E. coli*** **PotF**	***P. aeruginosa*** **SpuD**	***P. aeruginosa*** **SpuE**	***T. pallidum*** **TpPotD**	***Synechocystis*** **PotD**
SPD/PUT	PUT	PUT/SPD	SPD	PUT/SPD	SPD/PUT
Trp34	Trp37	Trp35	Trp34	Trp14	Leu40
Thr35	Ser38	Ser36	Thr35	Thr15	Asn41
Glu36	Asp39	Asp37	Asp36	Tyr16	ArgR42
Tyr37	Tyr40	Tyr38	Tyr37	Tyr17	Ser43
Tyr85	Ser85	Ser83	Asn84	Asp64	Leu113
Asp168	Ala182	Ser180	Ser178	Asp147	Asp206
Glu171	Glu185	Glu183	Glu181	Glu150	Glu209
Trp229	Trp244	Tyr241	Tyr239	Phe209	Trp267
Trp255	Phe276	Phe273	Trp271	Tyr238	Trp293
Asp257	Asp278	Asp275	Asp273	Asp240	Asp295
Tyr293	Tyr314	Phe311	Tyr309	Phe276	Ser329
Gln327	Leu348	Phe345	Ser343	Lys305	Leu363

Our co-workers produced recombinant *Synechocystis* PotD in *E. coli* as a His-tagged fusion protein. The protein was isolated from inclusion bodies, refolded and purified. The polyamine binding capacity and the spermidine preference of *Synechocystis* PotD was then demonstrated with a surface plasmon resonance binding experiment. No interactions with amino acids or polyamine derivatives (L-Arg, L-Glu, L-Asp, L-Lys, L-ornithine or cadaverine) were observed, therefore, the polyamine binding was specific. Furthermore, our co-workers showed that *Synechocystis* PotD indeed prefers binding spermidine over putrescine. Additionally, the role of PotD as a polyamine transporter was tested *in vivo* by the *Synechocystis potd* knock-out mutant. Spermidine uptake activity in the *potd* knock-out mutant was about 50 % lower than in the wild type, which indicated a significant role for *Synechocystis* PotD in spermidine transport. The remaining 50 % spermidine uptake activity suggests that there are other currently unidentified spermidine transporters in *Synechocystis*, whose role in spermidine uptake remains to be elucidated.

In publication III, polyamine binding studies using radioactive polyamines and recombinant *Synechocystis* PotD showed that *Synechocystis* PotD is capable of binding spermidine, putrescine as well as spermine. However, the affinity for putrescine was about two-fold lower than for spermidine, while the affinity for spermine was only slightly lower than for spermidine.

Docking studies were performed to clarify the preference of spermidine binding. The binding mode of the docked spermidine in the *Synechocystis* PotD model (Figure 11B and Supplementary Figure 3a in publication III) was very similar to the spermidine binding in *E. coli* PotD crystal structure (Figure 11A), which supported the reliability of docking. Even the largest of the docked polyamines, spermine, fitted well into the binding pocket and was placed along the same position as spermidine (Figure 11C and Supplementary Figure 3b in publication III). One additional residue, Gln71, interacted with the N14 nitrogen of spermine. A conserved water molecule (water 471 in *E. coli* PotF structure) was found to be important for the correct docking of putrescine. Consequently, it was added to the *Synechocystis* PotD model prior to performing the docking experiment. The binding mode of the docked putrescine was similar to the binding mode in the *E. coli* PotF structure and, therefore, water seems to mediate putrescine binding (Figure 11D and Supplementary Figure 3c in publication III).

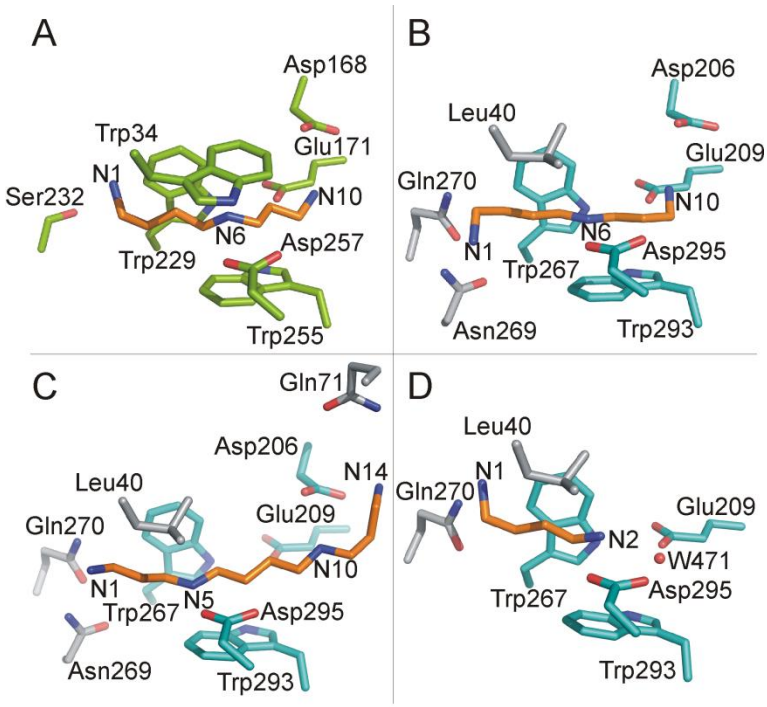

Figure 11. The spermidine binding site in *E. coli* PotD (A) (PDB ID: 1POT; Sugiyama *et al.* 1996b) and the docked binding mode of spermidine (B), spermine (C) and putrescine (D) in the *Synechocystis* PotD model. Binding residues in *E. coli* PotD are colored green. Conserved residues in *Synechocystis* PotD are colored cyan and non-conserved binding residues are colored gray. The polyamines are colored orange.

The crystal structures of *P. aeruginosa* SpuD and SpuE (Figure 4) are α/β type proteins, consisting of two similar globular domains (N and C domains) with the substrate binding site in a pocket between the domains (Wu *et al.* 2012). Comparison of SpuD-putrescine with PotF-putrescine and SpuE-spermidine with PotD-spermidine, revealed very similar structures with mean C^{α} RMSDs of 0.97 Å and 1.56 Å, respectively. Comparison of the *apo*-SpuD and *apo*-SpuE with the SpuD-putrescine and SpuE-spermidine, respectively, showed substantial differences in the relative orientation of the C domain in respect to the N domain, indicating that both SpuD and SpuE undergo large conformational changes when binding their respective ligands. Due to the large domain shifts, the ligand binding residues also shift from their position in the *apo*-form when the ligand is bound (Wu et al. 2012).

The sequence identity of *P. aeruginosa* SpuD and SpuE compared to *Synechocystis* PotD was 23 % and 24 %, respectively. The residues involved in binding putrescine in SpuD are well-conserved in PotF (Table 3) and even water molecules involved in ligand binding are conserved (Wu *et al.* 2012)

(Figure 4). In SpuE, most of the residues binding spermidine are conserved with *E. coli* PotD, however, some differences can be seen around the N3 atom of spermidine. For example, Gln327 in *E. coli* PotD interacts with spermidine N3 directly, while in *P. aeruginosa* SpuE the interaction of the corresponding residue Ser343 is mediated by a water molecule (Wu *et al.* 2012) (Table 3). In addition, Asp180 in SpuE binds spermidine N3 via the same water molecule, while in *E. coli* PotD no water is identified in the corresponding position and the corresponding residue (Arg170) does not bind spermidine at all. In *Synechocystis* PotD, the arginine is conserved (Arg208) indicating a similar binding mode for spermidine N3 as in *E. coli* PotD.

The *apo* and ligand-bound forms of SpuD and SpuE gave some insight into the structural determinants of the substrate specificity of the proteins. The water-mediated hydrogen bonds have previously been shown to be important for the putrescine specificity in *E. coli* PotF (Vassylyev *et al.* 1998). Wu *et al.* (2012) hypothesized that Glu181 in SpuE/Glu183 in SpuD together with Trp271 in SpuE/Phe273 in SpuD could be the key residues conferring substrate specificity. In spermidine-binding SpuE, Glu181 undergoes a large shift upon substrate binding, compared to the corresponding residue Glu183 in SpuD. Glu183, on the other hand, is able to form water-mediated hydrogen bonds with the bound putrescine together with Ser83. Due to the shift of Glu181 in SpuE, it would not be able to make similar water-mediated hydrogen bonds with putrescine (Wu *et al.* 2012). Additionally, Wu *et al.* (2012) showed by mutation of Trp271 in SpuE that a large hydrophobic residue favors the binding of spermidine and disfavors the presence of a water molecule needed for putrescine binding. In contrast, mutation of the corresponding residue in SpuD, Phe273, showed that a smaller aromatic residue together with the hydrogen bond formed by Glu183 favors putrescine binding, but still allows spermidine to bind with a lower affinity (Wu *et al.* 2012). The hypothesis could also be true for the other polyamine binding proteins, since the corresponding residues in spermidine-preferential *E. coli* and *Synechocystis* PotDs, are Trp255 and Trp293, respectively, while in putrescine-binding *E. coli* PotF and putrescine-preferential TpPotD the corresponding residues are Phe276 and Tyr238, respectively.

The genes encoding subunits of an ABC transporter are often arranged consecutively in an operon, hence the name ATP binding cassette transporter. However, in *Synechocystis* operons are less common than in other bacteria (Tomii and Kanehisa 1998). Another characteristic feature of ABC transporters in *Synechocystis* is that substrate binding proteins are fused to either permease subunits or to the ATPase (Tomii and Kanehisa 1998). So far, only the substrate binding PotD subunit of the polyamine transporter has been identified in *Synechocystis*, while the ATPase and the transmembrane subunits

have not been identified. BLAST searches with PotA, PotB and PotC sequences from other species did not reveal any clear candidates in *Synechocystis*. The sequence identities of the transmembrane subunits are presumably too low to be identified by similarity searches. In contrast, the ATPases have higher sequence identity and a few possible candidates were retrieved, however, further experimental studies are needed to clarify their identities.

Synechocystis PotD might also be part of a multifunction transporter, which shares the transmembrane and ATP binding subunits. Many of the ABC transporters in *E. coli* have multiple functions. Alternate genes encoding a particular transporter subunit can be expressed or repressed under different environmental conditions. For example, the prokaryotic type histidine and arginine importer share the transmembrane (HisQ and HisM) and NDB (HisP) subunits, while the substrate binding subunit is either the histidine-specific HisJ or the arginine-specific ArgT determining the function of the transporter (Moussatova *et al.* 2008).

4.4 The Flv2/Flv4 heterodimer from *Synechocystis* sp. strain PCC 6803

The FDP protein family is a group of modular proteins involved in O_2/NO detoxification in strict and facultative anaerobes. Many crystal structures have been solved of the FDPs, revealing a homodimer or homotetramer arrangement. The aim of the work in publication IV was to characterize the function and location of Flv2 and Flv4 from *Synechocystis* and to study the putative heterodimer formation of Flv2 and Flv4 by homology modeling. Previous results indicated a role in photoprotection of Flv2 and Flv4, which was further assessed.

Our co-workers showed in publication IV that Flv2 and Flv4 are coregulated, both at the transcript and protein levels and that the coregulation is independent of sll0218. In the absence of Flv2, Flv4 is strongly downregulated. Experiments with a *flag-flv4* strain showed the formation of the Flv2/FLAG-Flv4 heterodimer. FLAG-Flv4 did not form dimers in absence of Flv2. However, this can also be due to the interference of the FLAG-tag in dimer formation. Flv2, on the contrary, is able to form homodimers. However, when Flv4 is available for heterodimer formation, the amount of Flv2 homodimers is significantly decreased, which indicates preference for heterodimer formation.

4.4.1 The homology model of the Flv2/Flv4 heterodimer

In cyanobacteria, the FDPs consist of three structural domains. The β-lactamase-like domain containing the diiron center and the flavodoxin domain containing the FMN moiety are common for all FDPs, while the third flavin reductase domain has been found only in cyanobacterial and photosyntetic

eukaryotic FDPs so far. No crystal structures have been solved for a protein consisting of all three domains. Therefore, the homology models of the Flv2/Flv4 heterodimers consisted of the β-lactamase domain and the flavodoxin domain, while the flavin reductase domain was modeled separately.

Although the FDP family members share a sequence identity of only 30-40 %, they are known to have a similar 3D fold (Vicente *et al.* 2008a). To investigate the structural changes of the enzyme during electron transfer, the Flv2/Flv4 heterodimer was modeled in two different oxidation states based on the crystal structures of $F_{420}H_2$ oxidase from *M. marburgensis* (Seedorf *et al.* 2007): in the active reduced state with the switch loop in the closed conformation (PDB ID: 2OHI) and in the inactive oxidized state with the switch loop in the open conformation (PDB ID: 2OHJ). *M. marburgensis* $F_{420}H_2$ oxidase shares 29 % and 26 % sequence identity with *Synechocystis* Flv2 and Flv4, respectively. The Flv2/Flv4 heterodimer was also modeled based on the closed conformation of FprA from *M. thermoacetica* (PDB ID: 1YCF, Silaghi-Dumitrescu *et al.* 2003), with 26 % and 28 % sequence identity shared with *Synechocystis* Flv2 and Flv4, respectively.

The FMN and iron binding sites are located at the interface between the monomers. The Flv2/Flv4 heterodimer is formed in a head-to-tail arrangement, bringing the iron binding site of Flv2 close to the FMN binding site of Flv4 and *vice versa* (Figure 12). Based on our analysis, the binding site, which consists of the FMN binding site of the Flv2 monomer and the iron binding site of the Flv4 monomer is more conserved than the other binding site. The FMN binding site consists of six residues that are conserved or have been substituted by similar residues and the iron binding site is totally conserved (Figure 9A and 9B in publication IV). The other binding site, which consists of the FMN binding site of the Flv4 monomer and the iron binding site of the Flv2 monomer, is less conserved and does not seem to be functional.

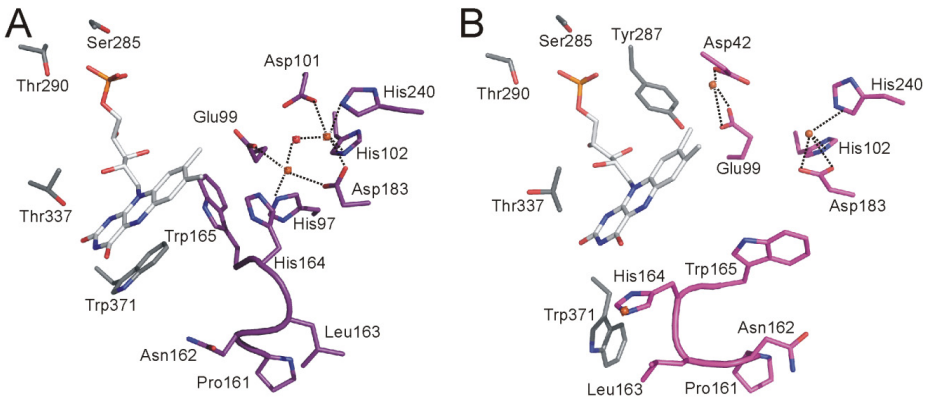

Figure 12. The FMN and diiron binding site of Flv2/Flv4 heterodimer in closed (A) and open (B) conformation. Only the conserved active site, with FMN binding site from Flv2 (gray) and diiron binding site from Flv4 (purple or magenta, respectively), is shown. Trp371 turns away from FMN (B), forming a cavity next to FMN in the open conformation.

Almost all members of the FDP family contain a conserved tryptophan residue in the FMN moiety. It is stacked at a 3.5 Å distance from the isoalloxazine of the FMN, shielding it from the solvent. The presence of the tryptophan residue blocks the FDP from accepting electrons directly from organic cofactors (Seedorf *et al.* 2007). In FDPs of methanogens and cyanobacteria, the tryptophan residue is replaced by a glycine. The presence of the glycine residue in the oxidized open conformation of *M. marburgensis* $F_{420}H_2$ oxidase (PDB ID: 2OHJ), allows parallell docking of the deazaisoalloxazine ring of the $F_{420}H_2$ in front of the FMN to allow electron transfer (Seedorf *et al.* 2007).

The tryptophan residue is conserved in Flv2 (Trp371) and *M. thermoacetica* FprA (Trp347), but similarly to *M. marburgensis* $F_{420}H_2$ oxidase, this residue is replaced by glycine in Flv4. The open and closed conformations of the Flv2/Flv4 model were compared in order to study the shift of the Trp371 in Flv2 (Figure 9 in publication IV). In the open conformation of the Flv2/Flv4 model, Trp371 is turned away from FMN and the second iron has made a 6 Å shift and is now coordinated by Asp42 and Glu99 from Flv4 and Tyr287 from Flv2 (Figure 12). Moreover, the open switch loop (161-Pro-Asn-Leu-His-164) is stabilized by a third iron at the protein surface, which causes Trp165 to move away from FMN creating a cavity next to FMN. The cavity formed next to the FMN in Flv4 is probably large enough to allow parallell docking of a cofactor in front of the FMN for electron transfer in a similar manner as in *M. marburgensis* $F_{420}H_2$ oxidase (Seedorf *et al.* 2007).

In experimental membrane subfractionation, Flv2 and Flv4 were found to strongly associate with the plasma membrane although no transmembrane

helices could be detected. By altering the buffers used in the experiments a strong cation dependency was shown. The electrostatic surface potential of the proposed Flv2/Flv4 heterodimer model indicated that Flv4 has a more negatively charged surface than Flv2. By comparison to crystal structures of related proteins, some conserved potential metal binding sites on the surface on the Flv2/Flv4 heterodimer model were identified, which could be responsible for the metal-dependent association between the heterodimer and the membrane.

4.4.2 The flavin reductase domain

The flavin reductase domain is able to directly link NADH oxidation to oxygen reduction, which shortens the reaction to one step instead of several, as in other flavoproteins (Vicente *et al.* 2002). The *Synechocystis* flavin reductase domain is able to bind either FMN or FAD (Vicente *et al.* 2002). Flv2 and Flv4 flavin reductase domains were modeled as separate monomers with bound FMN (Figure 8C in publication IV) based on the crystal structure of *Archaeoglobus fulgidus* ferric reductase (PDB ID: 1I0S, Chiu *et al.* 2001). The sequence identity between the template and Flv2 and Flv4 was 19 % and 22 %, respectively. The amino acids in the binding site are not conserved. However, FMN was bound mainly by main-chain interactions and the binding mode is similar to that of FMN in *A. fulgidus* ferric reductase.

4.4.3 Characterization of sll0218

The gene *sll0218*, which clusters together with *flv2* and *flv4* in the same operon in *Synechocystis*, was characterized. The sequence of sll0218 is highly conserved and was predicted to consist of four transmembrane helices by transmembrane prediction programs. A sequence analysis showed 47-71 % sequence identity of sll0218 to homologous proteins present in cyanobacteria (data not shown). In the experimental analysis of membranes in *Synechocystis* cells, sll0218 was found associated with a large membrane protein complex in the thylakoid membrane, while Flv2 and Flv4 reside in the cytoplasm or are associated with the plasma membrane. In cyanobacteria and higher plants PSII has been shown to form dimers (Hankamer *et al.* 1999; Kuhl *et al.* 2000). In mutants lacking sll0218 a decrease in PSII dimer complexes compared to PSII monomers could be seen, thus, sll0218 may function as a chaperone stabilizing the PSII dimer.

4.4.4 Flv2, sll0218 and Flv4 function in photoprotection of PSII

Flv2 and Flv4 was previously shown to function in the photoprotection of PSII (Zhang *et al.* 2009). The D1 protein synthesis was decreased in *flv2* and *flv4* deletion mutants compared to wild type or *flv1*/*flv3* deletion mutants. Thus,

the *flv2* and *flv4* deletion mutants were more susceptible to photoinhibition of PSII. These results indicated that Flv2 and Flv4 have a crucial role in preventing the production of ROS (Zhang *et al.* 2009). The results in publication IV show that the Flv2/Flv4 heterodimer is involved in electron traffic between the phycobiliosmes and PSII. Although located in different places of the cell, Flv2, sll0218 and Flv4 function together. Sll0218 is assumed to have a role in the assembly process and stabilizing of the PSII, while the Flv2/Flv4 heterodimer binds to the cytoplasmic side of the PSII and receives electrons from the Q_B site. Thus, Flv2/Flv4 participates in decreasing the high reduction level of the PQ pool and, therefore, decreasing the level of photodamage to PSII.

4.5 Reliability of the homology models

In this thesis, homology models for several different proteins are presented. Since the quality of the models highly depends on the sequence identity with the template structures, the reliability of the models varies. In order to make as accurate models as possible with the available structural data, careful thought was given to the projects throughout the modeling process, including literature and database searches, multiple sequence alignments as well as model building. Experimental work was done in combination with all modeling projects to support the models.

In publication I, the homology model of *Synechocystis* FutC had an overall sequence identity of 34 % with the template. The NBD, which binds ATP, shares 45 % sequence identity with the template structure and the NDB is the most reliable part of the model. ATP-binding is mediated by conserved motifs and the residues involved in binding ATP in *Synechocystis* FutC are conserved or substituted by similar residues. The regulatory domain had a sequence identity of only 18 % with the template and the model for this domain is, therefore, less reliable.

In publication II, a multiple sequence alignment consisting of the structures of *E. coli* PotD (Sugiyama *et al.* 1996a) and PotF (Vassylyev *et al.* 1998) and sequences of cyanobacterial polyamine transporters was used together with a secondary structure prediction for *Synechocystis* PotD in order to refine and improve the alignment. *Synechocystis* PotD had the highest overall sequence identity (24 %) with the structure of *E. coli* PotD (Sugiyama *et al.* 1996a). The model was evaluated with PROCHECK (Laskowski *et al.* 1993) and Prosa2003 (Sippl 1993). The sequence identity at the active site was high enough (38 %) to predict that *Synechocystis* PotD binds polyamines. The residues involved in binding polyamines in *E. coli* PotD (Sugiyama *et al.* 1996a) and PotF (Vassylyev *et al.* 1998) were known and *Synechocystis* PotD share more conserved residues with *E. coli* PotD than with PotF. In publication III, polyamine docking was made to the homology model of *Synechocystis* PotD. The quality of

docking depends on many factors e.g. the flexibility and quality of the ligand and protein structures, which was considered when evaluating the docking results and comparing them to the experimental work. Based on the literature, putrescine binding to *E. coli* PotF is mediated by a water molecule. In order to dock putrescine more reliably to the polyamine-binding site of *Synechocystis* PotD, the water molecule was added to the binding site before the putrescine docking experiment.

In publication IV, a similar approach to the multiple sequence alignment was taken as in the previous projects, namely the crystal structures of FDPs and sequences of putative flavoprotein sequences from cyanobacteria were included and data from the literature, for example the residues forming the active site, were used to refine the alignment. The Flv2/Flv4 heterodimer from *Synechocystis* was modeled in the open and closed conformations based on the *M. marburgenisis* $F_{420}H_2$ oxidase (Seedorf *et al.* 2007), which had the best overall sequence identity (29 % with Flv2 and 26 % with Flv4). In order to investigate the FMN-binding site more closely, the Flv2/Flv4 heterodimer was modeled based on the structure of FprA from *M. thermoacetica* (Silaghi-Dumitrescu *et al.* 2003), which has a sequence identity of 26 % with Flv2 and 28 % with Flv4. Additionally, Flv2 and Flv4 were modeled as homodimers in the closed conformation based on *M. marburgenisis* $F_{420}H_2$ oxidase (Seedorf *et al.* 2007) and homodimers were compared with the heterodimers in the analysis of the putative heterodimerization.

The C-terminal flavin reductase domains of Flv2 and Flv4 had a sequence identity of 19 % and 22 %, respectively, with the *Archaeoglobus fulgidus* ferric reductase structure (Chiu *et al.* 2001). The reliability of the models is, however, difficult to judge since FMN is bound mainly by main-chain interactions in the template structure and the residues involved in binding are not conserved among ferric reductase homologs (Chiu *et al.* 2001).

5 Conclusions

This thesis consist of the structural characterization of *Synechocystis* proteins from two different protein families, namely the ABC transporters and the flavodiiron proteins. Sequence analysis, homology modeling and ligand docking were used as methods to study the predicted structural features of FutC, PotD and the Flv2/Flv4 heterodimer.

Publication I describes the transcriptional regulation of the *fut* genes, encoding the ferric iron transporter $FutA_2BC$ in *Synechocystis*. The structural features of the ATPase subunit FutC and the ATP binding site was investigated using homology modeling. The NBD typically consists of conserved binding motifs and according to the model, ATP binding site would be highly conserved in *Synechocystis* FutC. In addition, the interaction of FutC with the transmembrane subunit FutB was investigated. FutB is divided into two homologous domains and the conserved EAA coupling motif is found in both domains. This indicates the possiblity to form salt bridges in a similar manner as in $MalGFK_2$, between the glutamate in the EAA motif and a conserved arginine residue in FutC. Taken together, the structural features that are critical for function and the interactions with FutB are conserved in the homology model of *Synechocystis* FutC.

In publication II, the *Synechocystis potd* gene was characterized for the first time and shown to be a functional gene. By constructing a homology model of PotD, the ability to bind polyamines and the preference for ligand were studied. Based on comparison with the crystal structures of *T. pallidum* TpPotD and *E. coli* PotD and PotF, *Synechocystis* PotD is more similar to the spermidine-preferential *E. coli* PotD, than to the putrescine binding PotF or TpPotD. My co-workers confirmed by experimental work the spermidine preference of *Synechocystis* PotD and, furthermore, that PotD has a physiological role in polyamine uptake.

In publication III, recombinant *Synechocystis* PotD was shown to have the highest affinity for spermidine, while a somewhat lower affinity for spermine and a two-fold lower affinity for putrescine. Polyamine docking studies were done to investigate the structural determinants for the polyamine binding specificity. The docking mode of spermidine to the *Synechocystis* PotD homology model followed the same pattern as the spermidine in *E. coli* PotD crystal structure and in the modeled spermidine-PotD complex. Spermine was positioned similarly as spermidine, while putrescine required a water molecule in the ligand binding pocket in order to dock correctly. In addition, Wu *et al.* showed that the key residues conferring substrate specifity in *P. aeruginosa* SpuD maintain water-mediated interactions with putrescine. Thus, the network of water-mediated interactions seem to be critical for putrescine

binding. In conclusion, *Synechocystis* PotD favours spermidine binding and seems to lack the prerequisite for a similar water-mediated network.

In publication IV, a novel type of photoprotection mechanism in cyanobacteria was presented. Experimental work with Flv2 and Flv4 in *Synechocystis* indicated that they function as a heterodimer, capable of rapid electron transfer between the FMN and diiron center. Homology models of *Synechocystis* Flv2 and Flv4 were constructed in order to study at the structural level whether Flv2 and Flv4 are capable of forming heterodimers and, additionally, to analyze the predicted structural features of the formed diiron and FMN binding sites. According to the heterodimer model one of the reactive sites is more conserved than the other and clearly functional. The functional reactive site of the heterodimer was compared to the Flv4 homodimer reactive site, in which the FMN binding residues are not fully conserved, and to the Flv2 homodimer reactive site, in which the iron binding residues are not fully conserved. Based on the comparison, the Flv2/Flv4 heterodimer has a structurally more conserved binding site than either of the homodimers, thus, supporting the heterodimer formation.

Furthermore, to investigate the structural changes of the enzyme during electron transfer, the Flv2/Flv4 heterodimer was modeled in two different oxidation states. The open conformation revealed displacement of the second iron and a cavity next to the FMN, indicating the possibility of docking cofactors parallel to the isoalloxazine ring and, moreover, direct electron transfer in a similar manner as in *M. marburgensis* $F_{420}H_2$ oxidase (Seedorf *et al.* 2007). The unknown protein sll0218, encoded in the *flv2-flv4* operon, is conserved among cyanobacteria and was proposed to function as a chaperone in the assembly of the PSII dimer, thereby facilitating the interaction of the Flv2/Flv4 heterodimer and energy transfer between PBS and PSII.

In conclusion, the structural analysis performed in this thesis revealed that FutC and PotD have the structural features needed for function. Furthermore, by sequence analysis and structural modeling combined with ligand docking, we revealed the structural basis for the substrate specificity of PotD. The structural analysis of Flv2/Flv4 supported the putative heterodimer formation and pinpointed the residues that constitute a functional reactive site.

References

Allahverdiyeva Y, Ermakova M, Eisenhut M, Zhang P, Richaud P, Hagemann M, Cournac L, Aro EM (2011) Interplay between flavodiiron proteins and photorespiration in Synechocystis sp. PCC 6803. J Biol Chem 286:24007-24014

Aller SG, Yu J, Ward A, Weng Y, Chittaboina S, Zhuo R, Harrell PM, Trinh YT, Zhang Q, Urbatsch IL, Chang G (2009) Structure of P-glycoprotein reveals a molecular basis for poly-specific drug binding. Science 323:1718-1722

Ambudkar SV, Kim IW, Xia D, Sauna ZE (2006) The A-loop, a novel conserved aromatic acid subdomain upstream of the Walker A motif in ABC transporters, is critical for ATP binding. FEBS Lett 580:1049-1055

Angerer A, Gaisser S, Braun V (1990) Nucleotide sequences of the sfuA, sfuB, and sfuC genes of Serratia marcescens suggest a periplasmic-binding-protein-dependent iron transport mechanism. J Bacteriol 172:572-578

Arnoux P, Haser R, Izadi-Pruneyre N, Lecroisey A, Czjzek M (2000) Functional aspects of the heme bound hemophore HasA by structural analysis of various crystal forms. Proteins 41:202-210

Arnoux P, Haser R, Izadi N, Lecroisey A, Delepierre M, Wandersman C, Czjzek M (1999) The crystal structure of HasA, a hemophore secreted by Serratia marcescens. Nat Struct Biol 6:516-520

Aro EM, Virgin I, Andersson B (1993) Photoinhibition of Photosystem II. Inactivation, protein damage and turnover. Biochim Biophys Acta 1143:113-134

Badarau A, Firbank SJ, Waldron KJ, Yanagisawa S, Robinson NJ, Banfield MJ, Dennison C (2008) Futa2 is a ferric binding protein from synechocystis PCC 6803. J Biol Chem 283:12520-12527

Berish SA, Mietzner TA, Mayer LW, Genco CA, Holloway BP, Morse SA (1990) Molecular cloning and characterization of the structural gene for the major iron-regulated protein expressed by Neisseria gonorrhoeae. J Exp Med 171:1535-1546

Berman HM, Westbrook J, Feng Z, Gilliland G, Bhat TN, Weissig H, Shindyalov IN, Bourne PE (2000) The Protein Data Bank. Nucleic Acids Res 28:235-242

Bouchereau A, Aziz A, Larher F, Martin-Tanguy J (1999) Polyamines environmental challenges, recent development. Plant Science 140:103-125

Bracken CS, Baer MT, Abdur-Rashid A, Helms W, Stojiljkovic I (1999) Use of heme-protein complexes by the Yersinia enterocolitica HemR receptor: histidine residues are essential for receptor function. J Bacteriol 181:6063-6072

Bruns CM, Anderson DS, Vaughan KG, Williams PA, Nowalk AJ, McRee DE, Mietzner TA (2001) Crystallographic and biochemical analyses of the metal-free Haemophilus influenzae Fe3+-binding protein. Biochemistry 40:15631-15637

Bruns CM, Nowalk AJ, Arvai AS, McTigue MA, Vaughan KG, Mietzner TA, McRee DE (1997) Structure of Haemophilus influenzae Fe(+3)-binding protein reveals convergent evolution within a superfamily. Nat Struct Biol 4:919-924

Buchan DW, Ward SM, Lobley AE, Nugent TC, Bryson K, Jones DT (2010) Protein annotation and modelling servers at University College London. Nucleic Acids Res 38:W563-8

Buchanan SK, Smith BS, Venkatramani L, Xia D, Esser L, Palnitkar M, Chakraborty R, van der Helm D, Deisenhofer J (1999)

Crystal structure of the outer membrane active transporter FepA from Escherichia coli. Nat Struct Biol 6:56-63

Cameron AD, Ridderstrom M, Olin B, Mannervik B (1999) Crystal structure of human glyoxalase II and its complex with a glutathione thiolester substrate analogue. Structure 7:1067-1078

Carfi A, Pares S, Duee E, Galleni M, Duez C, Frere JM, Dideberg O (1995) The 3-D structure of a zinc metallo-beta-lactamase from Bacillus cereus reveals a new type of protein fold. EMBO J 14:4914-4921

Cartron ML, Maddocks S, Gillingham P, Craven CJ, Andrews SC (2006) Feo--transport of ferrous iron into bacteria. Biometals 19:143-157

Chen J, Lu G, Lin J, Davidson AL, Quiocho FA (2003) A tweezers-like motion of the ATP-binding cassette dimer in an ABC transport cycle. Mol Cell 12:651-661

Chiu HJ, Johnson E, Schroder I, Rees DC (2001) Crystal structures of a novel ferric reductase from the hyperthermophilic archaeon Archaeoglobus fulgidus and its complex with NADP+. Structure 9:311-319

Chothia C, Lesk AM (1986) The relation between the divergence of sequence and structure in proteins. EMBO J 5:823-826

Clarke TE, Braun V, Winkelmann G, Tari LW, Vogel HJ (2002) X-ray crystallographic structures of the Escherichia coli periplasmic protein FhuD bound to hydroxamate-type siderophores and the antibiotic albomycin. J Biol Chem 277:13966-13972

Clarke TE, Ku SY, Dougan DR, Vogel HJ, Tari LW (2000) The structure of the ferric siderophore binding protein FhuD complexed with gallichrome. Nat Struct Biol 7:287-291

Das A, Coulter ED, Kurtz DM,Jr, Ljungdahl LG (2001) Five-gene cluster in Clostridium thermoaceticum consisting of two divergent operons encoding rubredoxin oxidoreductase- rubredoxin and rubrerythrin-type A flavoprotein- high-molecular-weight rubredoxin. J Bacteriol 183:1560-1567

Dau H, Zaharieva I, Haumann M (2012) Recent developments in research on water oxidation by photosystem II. Curr Opin Chem Biol 16:3-10

Dawson RJ, Locher KP (2007) Structure of the multidrug ABC transporter Sav1866 from Staphylococcus aureus in complex with AMP-PNP. FEBS Lett 581:935-938

Dawson RJ, Locher KP (2006) Structure of a bacterial multidrug ABC transporter. Nature 443:180-185

Di Matteo A, Scandurra FM, Testa F, Forte E, Sarti P, Brunori M, Giuffre A (2008) The O2-scavenging flavodiiron protein in the human parasite Giardia intestinalis. J Biol Chem 283:4061-4068

Doolittle RF (1990) Searching through sequence databases. Methods Enzymol 183:99-110

Doolittle RF, Johnson MS, Husain I, Van Houten B, Thomas DC, Sancar A (1986) Domainal evolution of a prokaryotic DNA repair protein and its relationship to active-transport proteins. Nature 323:451-453

Doolittle RF (1981) Protein evolution. Science 214:1123-1124

Ehrenreich IM, Waterbury JB, Webb EA (2005) Distribution and diversity of natural product genes in marine and freshwater cyanobacterial cultures and genomes. Appl Environ Microbiol 71:7401-7413

Ferguson AD, Chakraborty R, Smith BS, Esser L, van der Helm D, Deisenhofer J

(2002) Structural basis of gating by the outer membrane transporter FecA. Science 295:1715-1719

Ferreira KN, Iverson TM, Maghlaoui K, Barber J, Iwata S (2004) Architecture of the photosynthetic oxygen-evolving center. Science 303:1831-1838

Fitch WM (2000) Homology a personal view on some of the problems. Trends Genet 16:227-231

Frazão C, Silva G, Gomes CM, Matias P, Coelho R, Sieker L, Macedo S, Liu MY, Oliveira S, Teixeira M, Xavier AV, Rodrigues-Pousada C, Carrondo MA, Le Gall J (2000) Structure of a dioxygen reduction enzyme from Desulfovibrio gigas. Nat Struct Biol 7:1041-1045

Fulda S, Huang F, Nilsson F, Hagemann M, Norling B (2000) Proteomics of Synechocystis sp. strain PCC 6803. Identification of periplasmic proteins in cells grown at low and high salt concentrations. Eur J Biochem 267:5900-5907

Furuchi T, Kashiwagi K, Kobayashi H, Igarashi K (1991) Characteristics of the gene for a spermidine and putrescine transport system that maps at 15 min on the Escherichia coli chromosome. J Biol Chem 266:20928-20933

George AM, Jones PM (2012) Perspectives on the structure-function of ABC transporters: the Switch and Constant Contact models. Prog Biophys Mol Biol 109:95-107

Gerber S, Comellas-Bigler M, Goetz BA, Locher KP (2008) Structural basis of trans-inhibition in a molybdate/tungstate ABC transporter. Science 321:246-250

Gomes CM, Vicente JB, Wasserfallen A, Teixeira M (2000) Spectroscopic studies and characterization of a novel electron-transfer chain from Escherichia coli involving a flavorubredoxin and its flavoprotein reductase partner. Biochemistry 39:16230-16237

Gomes CM, Silva G, Oliveira S, LeGall J, Liu MY, Xavier AV, Rodrigues-Pousada C, Teixeira M (1997) Studies on the redox centers of the terminal oxidase from Desulfovibrio gigas and evidence for its interaction with rubredoxin. J Biol Chem 272:22502-22508

Groeger W, Koster W (1998) Transmembrane topology of the two FhuB domains representing the hydrophobic components of bacterial ABC transporters involved in the uptake of siderophores, haem and vitamin B12. Microbiology 144 (Pt 10):2759-2769

Groppa MD, Benavides MP (2008) Polyamines and abiotic stress: recent advances. Amino Acids 34:35-45

Guskov A, Kern J, Gabdulkhakov A, Broser M, Zouni A, Saenger W (2009) Cyanobacterial photosystem II at 2.9-A resolution and the role of quinones, lipids, channels and chloride. Nat Struct Mol Biol 16:334-342

Hankamer B, Morris EP, Barber J (1999) Revealing the structure of the oxygen-evolving core dimer of photosystem II by cryoelectron crystallography. Nat Struct Biol 6:560-564

Heby O, Emanuelsson H (1981) Role of the polyamines in germ cell differentiation and in early embryonic development. Med Biol 59:417-422

Helman Y, Tchernov D, Reinhold L, Shibata M, Ogawa T, Schwarz R, Ohad I, Kaplan A (2003) Genes encoding A-type flavoproteins are essential for photoreduction of O2 in cyanobacteria. Curr Biol 13:230-235

Higashi K, Sakamaki Y, Herai E, Demizu R, Uemura T, Saroj SD, Zenda R, Terui Y, Nishimura K, Toida T, Kashiwagi K, Igarashi K (2010) Identification and functions of amino acid residues in PotB and PotC involved in spermidine uptake activity. J Biol Chem 285:39061-39069

Higashi K, Ishigure H, Demizu R, Uemura T, Nishino K, Yamaguchi A, Kashiwagi K, Igarashi K (2008) Identification of a spermidine excretion protein complex (MdtJI) in Escherichia coli. J Bacteriol 190:872-878

Higgins CF, Linton KJ (2004) The ATP switch model for ABC transporters. Nat Struct Mol Biol 11:918-926

Higgins CF (1992) ABC transporters: from microorganisms to man. Annu Rev Cell Biol 8:67-113

Hohl M, Briand C, Grutter MG, Seeger MA (2012) Crystal structure of a heterodimeric ABC transporter in its inward-facing conformation. Nat Struct Mol Biol 19:395-402

Hollenstein K, Frei DC, Locher KP (2007a) Structure of an ABC transporter in complex with its binding protein. Nature 446:213-216

Hollenstein K, Dawson RJ, Locher KP (2007b) Structure and mechanism of ABC transporter proteins. Curr Opin Struct Biol 17:412-418

Huang F, Hedman E, Funk C, Kieselbach T, Schroder WP, Norling B (2004) Isolation of outer membrane of Synechocystis sp. PCC 6803 and its proteomic characterization. Mol Cell Proteomics 3:586-595

Huang L, McCluskey MP, Ni H, LaRossa RA (2002) Global gene expression profiles of the cyanobacterium Synechocystis sp. strain PCC 6803 in response to irradiation with UV-B and white light. J Bacteriol 184:6845-6858

Igarashi K, Kashiwagi K (2010) Characteristics of cellular polyamine transport in prokaryotes and eukaryotes. Plant Physiol Biochem 48:506-512

Igarashi K, Ito K, Kashiwagi K (2001) Polyamine uptake systems in Escherichia coli. Res Microbiol 152:271-278

Igarashi K, Kashiwagi K (1999) Polyamine transport in bacteria and yeast. Biochem J 344 Pt 3:633-642

Ikeuchi M, Tabata S (2001) Synechocystis sp. PCC 6803 - a useful tool in the study of the genetics of cyanobacteria. Photosynth Res 70:73-83

Izadi N, Henry Y, Haladjian J, Goldberg ME, Wandersman C, Delepierre M, Lecroisey A (1997) Purification and characterization of an extracellular heme-binding protein, HasA, involved in heme iron acquisition. Biochemistry 36:7050-7057

Johnson MS, Lehtonen JV (2000) . In: Higgins D, Taylor W (eds) Bioinformatics. Oxford University Press, United Kingdom, pp 15-50

Johnson MS, Srinivasan N, Sowdhamini R, Blundell TL (1994) Knowledge-based protein modeling. Crit Rev Biochem Mol Biol 29:1-68

Johnson MS, Overington JP (1993) A structural basis for sequence comparisons. An evaluation of scoring methodologies. J Mol Biol 233:716-738

Jones DT (1999) Protein secondary structure prediction based on position-specific scoring matrices. J Mol Biol 292:195-202

Jones G, Willett P, Glen RC, Leach AR, Taylor R (1997) Development and

validation of a genetic algorithm for flexible docking. J Mol Biol 267:727-748

Jones G, Willett P, Glen RC (1995) Molecular recognition of receptor sites using a genetic algorithm with a description of desolvation. J Mol Biol 245:43-53

Jones PM, George AM (2012) Role of the D-loops in allosteric control of ATP hydrolysis in an ABC transporter. J Phys Chem A 116:3004-3013

Kadaba NS, Kaiser JT, Johnson E, Lee A, Rees DC (2008) The high-affinity E. coli methionine ABC transporter: structure and allosteric regulation. Science 321:250-253

Kamiya N, Shen JR (2003) Crystal structure of oxygen-evolving photosystem II from Thermosynechococcus vulcanus at 3.7-A resolution. Proc Natl Acad Sci U S A 100:98-103

Kammler M, Schon C, Hantke K (1993) Characterization of the ferrous iron uptake system of Escherichia coli. J Bacteriol 175:6212-6219

Kaneko T, Sato S, Kotani H, Tanaka A, Asamizu E, Nakamura Y, Miyajima N, Hirosawa M, Sugiura M, Sasamoto S, Kimura T, Hosouchi T, Matsuno A, Muraki A, Nakazaki N, Naruo K, Okumura S, Shimpo S, Takeuchi C, Wada T, Watanabe A, Yamada M, Yasuda M, Tabata S (1996) Sequence analysis of the genome of the unicellular cyanobacterium Synechocystis sp. strain PCC6803. II. Sequence determination of the entire genome and assignment of potential protein-coding regions. DNA Res 3:109-136

Kashiwagi K, Innami A, Zenda R, Tomitori H, Igarashi K (2002) The ATPase activity and the functional domain of PotA, a component of the sermidine-preferential uptake system in Escherichia coli. J Biol Chem 277:24212-24219

Kashiwagi K, Kuraishi A, Tomitori H, Igarashi A, Nishimura K, Shirahata A, Igarashi K (2000) Identification of the putrescine recognition site on polyamine transport protein PotE. J Biol Chem 275:36007-36012

Kashiwagi K, Shibuya S, Tomitori H, Kuraishi A, Igarashi K (1997) Excretion and uptake of putrescine by the PotE protein in Escherichia coli. J Biol Chem 272:6318-6323

Kashiwagi K, Pistocchi R, Shibuya S, Sugiyama S, Morikawa K, Igarashi K (1996) Spermidine-preferential uptake system in Escherichia coli. Identification of amino acids involved in polyamine binding in PotD protein. J Biol Chem 271:12205-12208

Kashiwagi K, Miyamoto S, Suzuki F, Kobayashi H, Igarashi K (1992) Excretion of putrescine by the putrescine-ornithine antiporter encoded by the potE gene of Escherichia coli. Proc Natl Acad Sci U S A 89:4529-4533

Kashiwagi K, Suzuki T, Suzuki F, Furuchi T, Kobayashi H, Igarashi K (1991) Coexistence of the genes for putrescine transport protein and ornithine decarboxylase at 16 min on Escherichia coli chromosome. J Biol Chem 266:20922-20927

Katoh H, Hagino N, Grossman AR, Ogawa T (2001) Genes essential to iron transport in the cyanobacterium Synechocystis sp. strain PCC 6803. J Bacteriol 183:2779-2784

Katoh H, Grossman AR, Hagino N, Ogawa T (2000) A gene of Synechocystis sp. Strain PCC 6803 encoding a novel iron transporter. J Bacteriol 182:6523-6524

Kendrew JC, Bodo G, Dintzis HM, Parrish RG, Wykoff H, Phillips DC (1958) A three-dimensional model of the myoglobin molecule obtained by x-ray analysis. Nature 181:662-666

King GM, Garey MA (1999) Ferric iron reduction by bacteria associated with the roots of freshwater and marine macrophytes. Appl Environ Microbiol 65:4393-4398

Komenda J, Sobotka R, Nixon PJ (2012) Assembling and maintaining the Photosystem II complex in chloroplasts and cyanobacteria. Curr Opin Plant Biol 15:245-251

Komenda J, Barker M, Kuvikova S, de Vries R, Mullineaux CW, Tichy M, Nixon PJ (2006) The FtsH protease slr0228 is important for quality control of photosystem II in the thylakoid membrane of Synechocystis sp. PCC 6803. J Biol Chem 281:1145-1151

Koropatkin N, Randich AM, Bhattacharyya-Pakrasi M, Pakrasi HB, Smith TJ (2007) The structure of the iron-binding protein, FutA1, from Synechocystis 6803. J Biol Chem 282:27468-27477

Koster W (2001) ABC transporter-mediated uptake of iron, siderophores, heme and vitamin B12. Res Microbiol 152:291-301

Kranzler C, Lis H, Shaked Y, Keren N (2011) The role of reduction in iron uptake processes in a unicellular, planktonic cyanobacterium. Environ Microbiol 13:2990-2999

Krewulak KD, Vogel HJ (2008) Structural biology of bacterial iron uptake. Biochim Biophys Acta 1778:1781-1804

Krieg S, Huche F, Diederichs K, Izadi-Pruneyre N, Lecroisey A, Wandersman C, Delepelaire P, Welte W (2009) Heme uptake across the outer membrane as revealed by crystal structures of the receptor-hemophore complex. Proc Natl Acad Sci U S A 106:1045-1050

Krogh A, Larsson B, von Heijne G, Sonnhammer EL (2001) Predicting transmembrane protein topology with a hidden Markov model: application to complete genomes. J Mol Biol 305:567-580

Kuhl H, Kruip J, Seidler A, Krieger-Liszkay A, Bunker M, Bald D, Scheidig AJ, Rogner M (2000) Towards structural determination of the water-splitting enzyme. Purification, crystallization, and preliminary crystallographic studies of photosystem II from a thermophilic cyanobacterium. J Biol Chem 275:20652-20659

Kurihara S, Oda S, Kato K, Kim HG, Koyanagi T, Kumagai H, Suzuki H (2005) A novel putrescine utilization pathway involves gamma-glutamylated intermediates of Escherichia coli K-12. J Biol Chem 280:4602-4608

Kusano T, Berberich T, Tateda C, Takahashi Y (2008) Polyamines: essential factors for growth and survival. Planta 228:367-381

Lagergard T, Purven M, Frisk A (1993) Evidence of Haemophilus ducreyi adherence to and cytotoxin destruction of human epithelial cells. Microb Pathog 14:417-431

Laskowski RA, MacArthur MW, Moss DS, Thornton JM (1993) PROCHECK: a program to check the stereochemical quality of protein structures. J Appl Cryst 26:283-291

Lehtonen JV, Still DJ, Rantanen VV, Ekholm J, Bjorklund D, Iftikhar Z, Huhtala M, Repo S, Jussila A, Jaakkola J, Pentikainen O, Nyronen T, Salminen T, Gyllenberg M, Johnson MS (2004) BODIL: a molecular modeling environment for structure-function analysis and drug design. J Comput Aided Mol Des 18:401-419

Lesuisse E, Labbe P (1989) Reductive and non-reductive mechanisms of iron assimilation by the yeast Saccharomyces cerevisiae. J Gen Microbiol 135:257-263

Letoffe S, Delepelaire P, Wandersman C (2004) Free and hemophore-bound heme

acquisitions through the outer membrane receptor HasR have different requirements for the TonB-ExbB-ExbD complex. J Bacteriol 186:4067-4074

Locher KP, Lee AT, Rees DC (2002) The E. coli BtuCD structure: a framework for ABC transporter architecture and mechanism. Science 296:1091-1098

Locher KP, Rees B, Koebnik R, Mitschler A, Moulinier L, Rosenbusch JP, Moras D (1998) Transmembrane signaling across the ligand-gated FhuA receptor: crystal structures of free and ferrichrome-bound states reveal allosteric changes. Cell 95:771-778

Lu CD, Itoh Y, Nakada Y, Jiang Y (2002) Functional analysis and regulation of the divergent spuABCDEFGH-spuI operons for polyamine uptake and utilization in Pseudomonas aeruginosa PAO1. J Bacteriol 184:3765-3773

Machius M, Brautigam CA, Tomchick DR, Ward P, Otwinowski Z, Blevins JS, Deka RK, Norgard MV (2007) Structural and biochemical basis for polyamine binding to the Tp0655 lipoprotein of Treponema pallidum: putative role for Tp0655 (TpPotD) as a polyamine receptor. J Mol Biol 373:681-694

Mehler AH (1951) Studies on reactions of illuminated chloroplasts. I. Mechanism of the reduction of oxygen and other Hill reagents. Arch Biochem Biophys 33:65-77

Michel KP, Pistorius EK (2004) Adaptation of the photosynthetic electron transport chain in cyanobacteria to iron deficiency: The function of IdiA and IsiA. Physiol Plant 120:36-50

Morrissey J, Guerinot ML (2009) Iron uptake and transport in plants: the good, the bad, and the ionome. Chem Rev 109:4553-4567

Moussatova A, Kandt C, O'Mara ML, Tieleman DP (2008) ATP-binding cassette transporters in Escherichia coli. Biochim Biophys Acta 1778:1757-1771

Nakao M, Okamoto S, Kohara M, Fujishiro T, Fujisawa T, Sato S, Tabata S, Kaneko T, Nakamura Y (2010) CyanoBase: the cyanobacteria genome database update 2010. Nucleic Acids Res 38:D379-81

Nicolaisen K, Moslavac S, Samborski A, Valdebenito M, Hantke K, Maldener I, Muro-Pastor AM, Flores E, Schleiff E (2008) Alr0397 is an outer membrane transporter for the siderophore schizokinen in Anabaena sp. strain PCC 7120. J Bacteriol 190:7500-7507

Nishiyama Y, Allakhverdiev SI, Murata N (2006) A new paradigm for the action of reactive oxygen species in the photoinhibition of photosystem II. Biochim Biophys Acta 1757:742-749

Nixon PJ, Michoux F, Yu J, Boehm M, Komenda J (2010) Recent advances in understanding the assembly and repair of photosystem II. Ann Bot 106:1-16

Nixon PJ, Barker M, Boehm M, de Vries R, Komenda J (2005) FtsH-mediated repair of the photosystem II complex in response to light stress. J Exp Bot 56:357-363

Niyogi KK (1999) PHOTOPROTECTION REVISITED: Genetic and Molecular Approaches. Annu Rev Plant Physiol Plant Mol Biol 50:333-359

Oldham ML, Chen J (2011a) Crystal structure of the maltose transporter in a pretranslocation intermediate state. Science 332:1202-1205

Oldham ML, Chen J (2011b) Snapshots of the maltose transporter during ATP hydrolysis. Proc Natl Acad Sci U S A 108:15152-15156

Oldham ML, Khare D, Quiocho FA, Davidson AL, Chen J (2007) Crystal structure of a catalytic intermediate of the maltose transporter. Nature 450:515-521

Packham G, Cleveland JL (1994) Ornithine decarboxylase is a mediator of c-Myc-induced apoptosis. Mol Cell Biol 14:5741-5747

Pejchal R, Sargeant R, Ludwig ML (2005) Structures of NADH and CH3-H4folate complexes of Escherichia coli methylenetetrahydrofolate reductase reveal a spartan strategy for a ping-pong reaction. Biochemistry 44:11447-11457

Perkins-Balding D, Ratliff-Griffin M, Stojiljkovic I (2004) Iron transport systems in Neisseria meningitidis. Microbiol Mol Biol Rev 68:154-171

Pinkett HW, Lee AT, Lum P, Locher KP, Rees DC (2007) An inward-facing conformation of a putative metal-chelate-type ABC transporter. Science 315:373-377

Pistocchi R, Kashiwagi K, Miyamoto S, Nukui E, Sadakata Y, Kobayashi H, Igarashi K (1993) Characteristics of the operon for a putrescine transport system that maps at 19 minutes on the Escherichia coli chromosome. J Biol Chem 268:146-152

Raksajit W, Yodsang P, Maenpaa P, Incharoensakdi A (2009) Characterization of spermidine transport system in a cyanobacterium,synechocystis sp. PCC 6803. J Microbiol Biotechnol 19:447-454

Raksajit W, Maenpaa P, Incharoensakdi A (2006) Putrescine transport in a cyanobacterium Synechocystis sp. PCC 6803. J Biochem Mol Biol 39:394-399

Rexroth S, Mullineaux CW, Ellinger D, Sendtko E, Rogner M, Koenig F (2011) The plasma membrane of the cyanobacterium Gloeobacter violaceus contains segregated bioenergetic domains. Plant Cell 23:2379-2390

Rohde KH, Gillaspy AF, Hatfield MD, Lewis LA, Dyer DW (2002) Interactions of haemoglobin with the Neisseria meningitidis receptor HpuAB: the role of TonB and an intact proton motive force. Mol Microbiol 43:335-354

Rost B, Yachdav G, Liu J (2004) The PredictProtein server. Nucleic Acids Res 32:W321-6

Sali A, Blundell TL (1993) Comparative protein modelling by satisfaction of spatial restraints. J Mol Biol 234:779-815

Scheffel F, Demmer U, Warkentin E, Hulsmann A, Schneider E, Ermler U (2005) Structure of the ATPase subunit CysA of the putative sulfate ATP-binding cassette (ABC) transporter from Alicyclobacillus acidocaldarius. FEBS Lett 579:2953-2958

Schryvers AB, Stojiljkovic I (1999) Iron acquisition systems in the pathogenic Neisseria. Mol Microbiol 32:1117-1123

Seedorf H, Hagemeier CH, Shima S, Thauer RK, Warkentin E, Ermler U (2007) Structure of coenzyme F420H2 oxidase (FprA), a di-iron flavoprotein from methanogenic Archaea catalyzing the reduction of O2 to H2O. FEBS J 274:1588-1599

Seedorf H, Dreisbach A, Hedderich R, Shima S, Thauer RK (2004) F420H2 oxidase (FprA) from Methanobrevibacter arboriphilus, a coenzyme F420-dependent enzyme involved in O2 detoxification. Arch Microbiol 182:126-137

Seiler N, Raul F (2005) Polyamines and apoptosis. J Cell Mol Med 9:623-642

Shouldice SR, Dougan DR, Skene RJ, Tari LW, McRee DE, Yu RH, Schryvers AB (2003a) High resolution structure of an alternate form of the ferric ion binding

protein from Haemophilus influenzae. J Biol Chem 278:11513-11519

Shouldice SR, Dougan DR, Williams PA, Skene RJ, Snell G, Scheibe D, Kirby S, Hosfield DJ, McRee DE, Schryvers AB, Tari LW (2003b) Crystal structure of Pasteurella haemolytica ferric ion-binding protein A reveals a novel class of bacterial iron-binding proteins. J Biol Chem 278:41093-41098

Silaghi-Dumitrescu R, Kurtz DM,Jr, Ljungdahl LG, Lanzilotta WN (2005) X-ray crystal structures of Moorella thermoacetica FprA. Novel diiron site structure and mechanistic insights into a scavenging nitric oxide reductase. Biochemistry 44:6492-6501

Silaghi-Dumitrescu R, Coulter ED, Das A, Ljungdahl LG, Jameson GN, Huynh BH, Kurtz DM,Jr (2003) A flavodiiron protein and high molecular weight rubredoxin from Moorella thermoacetica with nitric oxide reductase activity. Biochemistry 42:2806-2815

Silva P, Thompson E, Bailey S, Kruse O, Mullineaux CW, Robinson C, Mann NH, Nixon PJ (2003) FtsH is involved in the early stages of repair of photosystem II in Synechocystis sp PCC 6803. Plant Cell 15:2152-2164

Simpson LM, Oliver JD (1993) Regulation of proteolytic activity of Vibrio vulnificus by iron-containing compounds. Microb Pathog 14:249-252

Sippl MJ (1993) Recognition of errors in three-dimensional structures of proteins. Proteins 17:355-362

Smutna T, Goncalves VL, Saraiva LM, Tachezy J, Teixeira M, Hrdy I (2009) Flavodiiron protein from Trichomonas vaginalis hydrogenosomes: the terminal oxygen reductase. Eukaryot Cell 8:47-55

Soksawatmaekhin W, Kuraishi A, Sakata K, Kashiwagi K, Igarashi K (2004) Excretion and uptake of cadaverine by CadB and its physiological functions in Escherichia coli. Mol Microbiol 51:1401-1412

Srivastava R, Pisareva T, Norling B (2005) Proteomic studies of the thylakoid membrane of Synechocystis sp. PCC 6803. Proteomics 5:4905-4916

Stintzi A, Barnes C, Xu J, Raymond KN (2000) Microbial iron transport via a siderophore shuttle: a membrane ion transport paradigm. Proc Natl Acad Sci U S A 97:10691-10696

Stoebner JA, Payne SM (1988) Iron-regulated hemolysin production and utilization of heme and hemoglobin by Vibrio cholerae. Infect Immun 56:2891-2895

Stojiljkovic I, Larson J, Hwa V, Anic S, So M (1996) HmbR outer membrane receptors of pathogenic Neisseria spp.: iron-regulated, hemoglobin-binding proteins with a high level of primary structure conservation. J Bacteriol 178:4670-4678

Sugiyama S, Vassylyev DG, Matsushima M, Kashiwagi K, Igarashi K, Morikawa K (1996a) Crystal structure of PotD, the primary receptor of the polyamine transport system in Escherichia coli. J Biol Chem 271:9519-9525

Sugiyama S, Matsuo Y, Maenaka K, Vassylyev DG, Matsushima M, Kashiwagi K, Igarashi K, Morikawa K (1996b) The 1.8-A X-ray structure of the Escherichia coli PotD protein complexed with spermidine and the mechanism of polyamine binding. Protein Sci 5:1984-1990

Thomas T, Thomas TJ (2001) Polyamines in cell growth and cell death: molecular mechanisms and therapeutic applications. Cell Mol Life Sci 58:244-258

Tölle J, Michel KP, Kruip J, Kahmann U, Preisfeld A, Pistorius EK (2002) Localization and function of the IdiA homologue Slr1295 in the cyanobacterium Synechocystis sp. strain PCC 6803. Microbiology 148:3293-3305

Tomii K, Kanehisa M (1998) A comparative analysis of ABC transporters in complete microbial genomes. Genome Res 8:1048-1059

Tomitori H, Kashiwagi K, Igarashi K (2012) Structure and function of polyamine-amino acid antiporters CadB and PotE in Escherichia coli. Amino Acids 42:733-740

Tomitori H, Kashiwagi K, Asakawa T, Kakinuma Y, Michael AJ, Igarashi K (2001) Multiple polyamine transport systems on the vacuolar membrane in yeast. Biochem J 353:681-688

Tom-Yew SA, Cui DT, Bekker EG, Murphy ME (2005) Anion-independent iron coordination by the Campylobacter jejuni ferric binding protein. J Biol Chem 280:9283-9290

Tramontano A (1998) Homology modeling with low sequence identity. Methods 14:293-300

Tyystjärvi E (2013) Photoinhibition of photosystem II. In: Jeon K (ed) International Review Of Cell and Molecular Biology. Academic Press, Elsevier Inc., pp. 243–303

Umena Y, Kawakami K, Shen JR, Kamiya N (2011) Crystal structure of oxygen-evolving photosystem II at a resolution of 1.9 A. Nature 473:55-60

UniProt Consortium (2012) Reorganizing the protein space at the Universal Protein Resource (UniProt). Nucleic Acids Res 40:D71-5

Vassylyev DG, Tomitori H, Kashiwagi K, Morikawa K, Igarashi K (1998) Crystal structure and mutational analysis of the Escherichia coli putrescine receptor. Structural basis for substrate specificity. J Biol Chem 273:17604-17609

Verdon G, Albers SV, Dijkstra BW, Driessen AJ, Thunnissen AM (2003) Crystal structures of the ATPase subunit of the glucose ABC transporter from Sulfolobus solfataricus: nucleotide-free and nucleotide-bound conformations. J Mol Biol 330:343-358

Vicente JB, Carrondo MA, Teixeira M, Frazão C (2008a) Structural studies on flavodiiron proteins. Methods Enzymol 437:3-19

Vicente JB, Justino MC, Goncalves VL, Saraiva LM, Teixeira M (2008b) Biochemical, spectroscopic, and thermodynamic properties of flavodiiron proteins. Methods Enzymol 437:21-45

Vicente JB, Scandurra FM, Forte E, Brunori M, Sarti P, Teixeira M, Giuffre A (2008c) Kinetic characterization of the Escherichia coli nitric oxide reductase flavorubredoxin. Methods Enzymol 437:47-62

Vicente JB, Teixeira M (2005) Redox and spectroscopic properties of the Escherichia coli nitric oxide-detoxifying system involving flavorubredoxin and its NADH-oxidizing redox partner. J Biol Chem 280:34599-34608

Vicente JB, Gomes CM, Wasserfallen A, Teixeira M (2002) Module fusion in an A-type flavoprotein from the cyanobacterium Synechocystis condenses a multiple-component pathway in a single polypeptide chain. Biochem Biophys Res Commun 294:82-87

Wandersman C, Delepelaire P (2004) Bacterial iron sources: from siderophores

to hemophores. Annu Rev Microbiol 58:611-647

Ward A, Reyes CL, Yu J, Roth CB, Chang G (2007) Flexibility in the ABC transporter MsbA: Alternating access with a twist. Proc Natl Acad Sci U S A 104:19005-19010

Warkentin E, Mamat B, Sordel-Klippert M, Wicke M, Thauer RK, Iwata M, Iwata S, Ermler U, Shima S (2001) Structures of F420H2:NADP+ oxidoreductase with and without its substrates bound. EMBO J 20:6561-6569

Wasserfallen A, Ragettli S, Jouanneau Y, Leisinger T (1998) A family of flavoproteins in the domains Archaea and Bacteria. Eur J Biochem 254:325-332

Wu D, Lim SC, Dong Y, Wu J, Tao F, Zhou L, Zhang LH, Song H (2012) Structural basis of substrate binding specificity revealed by the crystal structures of polyamine receptors SpuD and SpuE from Pseudomonas aeruginosa. J Mol Biol 416:697-712

Yin L, Fristedt R, Herdean A, Solymosi K, Bertrand M, Andersson MX, Mamedov F, Vener AV, Schoefs B, Spetea C (2012) Photosystem II function and dynamics in three widely used Arabidopsis thaliana accessions. PLoS One 7:e46206

Zang TM, Hollman DA, Crawford PA, Crowder MW, Makaroff CA (2001) Arabidopsis glyoxalase II contains a zinc/iron binuclear metal center that is essential for substrate binding and catalysis. J Biol Chem 276:4788-4795

Zhang L, Paakkarinen V, van Wijk KJ, Aro EM (1999) Co-translational assembly of the D1 protein into photosystem II. J Biol Chem 274:16062-16067

Zhang P, Allahverdiyeva Y, Eisenhut M, Aro EM (2009) Flavodiiron proteins in oxygenic photosynthetic organisms: photoprotection of photosystem II by Flv2 and Flv4 in Synechocystis sp. PCC 6803. PLoS One 4:e5331

Zouni A, Witt HT, Kern J, Fromme P, Krauss N, Saenger W, Orth P (2001) Crystal structure of photosystem II from Synechococcus elongatus at 3.8 A resolution. Nature 409:739-743

ISBN 978-952-12-2886-5